



Loading and fate of particulate organic carbon from the Himalaya to the Ganga–Brahmaputra delta

Valier Galy, Christian France-Lanord, Bruno Lartiges

► To cite this version:

Valier Galy, Christian France-Lanord, Bruno Lartiges. Loading and fate of particulate organic carbon from the Himalaya to the Ganga–Brahmaputra delta. *Geochimica et Cosmochimica Acta*, 2008, 72 (7), pp.1767-1787. 10.1016/j.gca.2008.01.027 . hal-02364229

HAL Id: hal-02364229

<https://hal.univ-lorraine.fr/hal-02364229>

Submitted on 14 Nov 2019

HAL is a multi-disciplinary open access archive for the deposit and dissemination of scientific research documents, whether they are published or not. The documents may come from teaching and research institutions in France or abroad, or from public or private research centers.

L'archive ouverte pluridisciplinaire **HAL**, est destinée au dépôt et à la diffusion de documents scientifiques de niveau recherche, publiés ou non, émanant des établissements d'enseignement et de recherche français ou étrangers, des laboratoires publics ou privés.

Accepted Manuscript

Loading and fate of particulate organic carbon from the Himalaya to the Ganga-Brahmaputra delta

Valier Galy, Christian France-Lanord, Bruno Lartiges

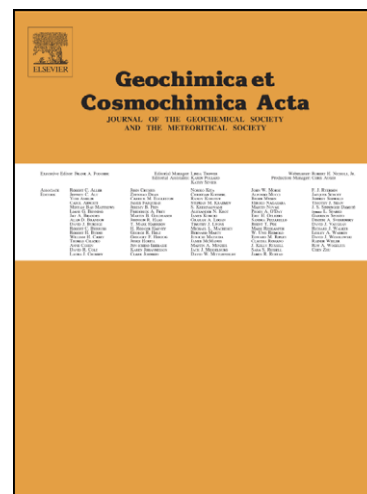
PII: S0016-7037(08)00061-6
DOI: [10.1016/j.gca.2008.01.027](https://doi.org/10.1016/j.gca.2008.01.027)
Reference: GCA 5542

To appear in: *Geochimica et Cosmochimica Acta*

Received Date: 25 April 2007
Accepted Date: 29 January 2008

Please cite this article as: Galy, V., France-Lanord, C., Lartiges, B., Loading and fate of particulate organic carbon from the Himalaya to the Ganga-Brahmaputra delta, *Geochimica et Cosmochimica Acta* (2008), doi: [10.1016/j.gca.2008.01.027](https://doi.org/10.1016/j.gca.2008.01.027)

This is a PDF file of an unedited manuscript that has been accepted for publication. As a service to our customers we are providing this early version of the manuscript. The manuscript will undergo copyediting, typesetting, and review of the resulting proof before it is published in its final form. Please note that during the production process errors may be discovered which could affect the content, and all legal disclaimers that apply to the journal pertain.



Loading and fate of particulate organic carbon from the Himalaya to the Ganga-Brahmaputra delta

Valier Galy^{1*}, Christian France-Lanord¹, Bruno Lartiges²

1 - Nancy Université, CRPG CNRS/INSU, BP 20, 54501 Vandœuvre-lès-Nancy, France.

2 - Nancy Université, LEM CNRS/INSU, BP 40, 54501 Vandœuvre-lès-Nancy, France

* Corresponding author, present address: Woods Hole Oceanographic Institution, Department
of Marine Chemistry and Geochemistry, Woods Hole, MA 02543, USA.

e-mail: vgaly@whoi.edu

ABSTRACT

We use the evolution of river sediment characteristics and sedimentary C_{org} from the Himalayan range to the delta to study the transport of C_{org} in the Ganga-Brahmaputra system and especially its fate during floodplain transit.

A detailed characterisation of both mineral and organic particles for a sampling set of river sediments allows taking into account the sediment heterogeneity characteristic of such large rivers. We study the relationships between sediment characteristics (mineralogy, grain size, specific area) and C_{org} content in order to evaluate the controls on C_{org} loading. Contributions of C3 and C4 plants are estimated from C_{org} stable isotopic composition ($\delta^{13}C_{org}$). We use the evolution of $\delta^{13}C_{org}$ values from the Himalayan range to the delta in order to study the fate of C_{org} during floodplain transit.

Ganga and Brahmaputra sediments define two distinct linear relations with specific area. In spite of 4 to 5 times higher specific area, Ganga sediments have similar C_{org} content, grain size and mineralogy as Brahmaputra sediments, indicating that specific area does not exert a primary control on C_{org} loading. The general correlation between the total C_{org} content and Al/Si ratio indicates that C_{org} loading is mainly related to: (1) segregation of organic particles under hydrodynamic forces in the river and, (2) the ability of mineral particles to form organo-mineral aggregates.

Bed and suspended sediments have distinct $\delta^{13}C_{org}$ values. In bed sediments, $\delta^{13}C_{org}$ values are compatible with a dominant proportion of fossil C_{org} derived from Himalayan rocks erosion. Suspended sediments from Himalayan tributaries at the outflow of the range have low $\delta^{13}C_{org}$ values (-24.8 ‰ average) indicating a dominant proportion of C3 plant inputs. In the Brahmaputra basin, $\delta^{13}C_{org}$ values of suspended sediments are constant along the river course in the plain. On the contrary, suspended sediments of the Ganga in Bangladesh have higher

$\delta^{13}\text{C}_{\text{org}}$ values (-22.4 to -20.0 ‰), consistent with a significant contribution of C4 plant derived from the floodplain. Our data indicate that, during the plain transit, more than 50 % of the recent biogenic C_{org} coming from the Himalaya is oxidised and replaced by floodplain C_{org} . This renewal process likely occurs during successive deposition-erosion cycles and river course avulsions in the plain.

1. INTRODUCTION

Interactions between atmosphere, ocean and continent determine both the shape and climate of the Earth's surface through a sequence of complex processes. Rivers play an important role in this interplay since they are the main conveyors of elements from the continents to the ocean, carrying both mineral and organic species as dissolved and particulate phases. Their role in the long-term climate regulation has long been highlighted and debated, especially through the transport of dissolved cations derived from silicate weathering (GAILLARDET et al., 1999; RUDDIMAN, 1997 and ref. therein). More recently, organic carbon (C_{org}) transport by rivers has also been receiving more and more attention. Indeed, rivers transport particulate C_{org} to the ocean that if buried represents a net sink of atmospheric CO_2 , and participates in the long-term climate regulation (e.g. LASAGA et al., 1985; SUNDQUIST, 1985). Nevertheless, rivers appear to export a minor proportion of the net primary production since ca. 99% is oxidised to CO_2 in soils and returns to the atmosphere (MACKENZIE, 1981). The fate of riverine C_{org} in the oceanic system was also extensively studied as the proportion of riverine C_{org} that is preserved determines the extent of the CO_2 sequestration (e.g. GONI et al., 2006; HEDGES et al., 1997). Actually, C_{org} mineralization in the ocean considerably reduces the C_{org} burial flux and, at the global scale, ca. 70% of riverine C_{org} is oxidised prior to being buried in sediments (BURDIGE, 2005; HEDGES et al., 1997; LUDWIG et al., 1996; SCHLÜNZ and SCHNEIDER, 2000). The role of rivers in terrestrial C_{org} export and burial appears to be more complex than a simple conveyor as it also has a great impact on both the flux and the composition of terrestrial C_{org} and thus on its behaviour. This is highlighted by the contrast between different river systems in terms of terrestrial C_{org} flux, composition and preservation in the ocean. For instance, a large river system with well-developed floodplain such as the Amazon appears to have a C_{org} transport dynamic that is completely different from that of

small mountainous rivers such as New Zealand rivers, Taiwanese rivers and the Eel river where the transport is very direct from the continent to the ocean (e.g. AUFDENKAMPE et al., 2007; BLAIR et al., 2004; HILTON et al., in press; SCOTT et al., 2006). Understanding the controls of C_{org} loading, composition and fate during the fluvial transport is therefore crucial to address the role of continental erosion in the global carbon cycle.

Himalayan erosion generates the largest sediment flux from a single continental drainage basin to the ocean. Each year 1 to 2 billion tons of particles are transported by the Ganga-Brahmaputra (G-B) fluvial system from the Himalayan range to the Bay of Bengal and deposited in the Bengal Fan turbiditic system. The global importance of C_{org} flux associated with sediment transport in the G-B fluvial system has been highlighted in previous studies on the basis of the modern river or the sedimentary record characterisations (AUCOUR et al., 2006; FRANCE-LANORD and DERRY, 1997; SUBRAMANIAN and ITTEKKOT, 1991). Recently, we realised a comprehensive budget of C_{org} from Himalayan rocks to the Bengal Fan showing that modern burial flux of recent C_{org} generated by Himalayan erosion is $3.1 \pm 0.3 \times 10^{11}$ mol/yr and represents ca. 15 % of the global flux (GALY et al., 2007b). In addition, we discovered that the Himalayan system is characterised by an extreme C_{org} burial efficiency, since almost 100 % of C_{org} exported by G-B fluvial system is effectively buried in Bengal Fan sediments. This gives the G-B fluvial system a determinant role in terms of terrestrial C_{org} exportation and burial, and therefore in terms of atmospheric CO_2 sequestration.

In this paper we present a detailed characterisation of both C_{org} and mineral particles transported by rivers from the base of the Himalayan range to the G-B delta. We developed and used a depth profile sampling procedure which allowed the large sediment heterogeneity occurring in such rivers to be taken into account (GALY et al., 2007b; SINGH and FRANCE-

LANORD, 2002). Total C_{org} content (TOC^+) and stable isotopic composition ($\delta^{13}C_{org}$) as well as major element compositions (Al and Si), grain size and specific area are reported for the set of river sediments. Thanks to the wide range of sediment properties, the comparison between C_{org} content and bulk sediment physical properties allows study of their respective control on C_{org} loading. The role of specific area, mineralogy and grain size, three significant parameters (e.g. SOLLINS et al., 1996), is especially discussed. To define average C_{org} loading in these sediments, we use the normalisation to a chemical parameter (Al/Si) integrating several sorting processes such as grain size and mineralogy. $\delta^{13}C$ of bulk organic matter is used to evaluate the source and nature of C_{org} , especially the relative contributions of C3 and C4 plants. Following the evolution of both C_{org} loading and composition from the base of the range to the delta allows study of the fate of C_{org} during its transport throughout the fluvial system and especially highlights the role of the floodplain. Detailed study of the Himalayan system therefore provides insights on two critical issues: (1) what controls C_{org} loading in river sediments? and, (2) what is the fate of particulate C_{org} during fluvial transport, i.e. does a river act as a simple conveyor or as a reactor?

2. MATERIAL AND METHODS

2.1 Sampling strategy

The Ganga-Brahmaputra (G-B) basin can be divided in two distinct geomorphic parts: (1) the Himalayan range characterised by steep slopes and high incision, and (2) the floodplain characterised by flat topography and drained by very large rivers. The transition between the two sub-units is abrupt as the slope of the rivers decrease by several orders of magnitude

within a few kilometres. The Himalayan range is drained southward by a dozen Trans-Himalayan rivers originating in southern Tibet, which collects most of the Himalayan runoff and supply G-B in the East-West Indo-Gangetic floodplain. The G-B basin is composed of two sub-basins: the Ganga basin to the West and the Brahmaputra basin to the East. The Himalayan part of these two sub-basins are quite comparable but their floodplains are very different. The Ganga floodplain is 200 to 300 km wide and very flat with the Ganga meandering far south of the Himalayan front. On the other hand, the Brahmaputra floodplain is only 50 to 100 km wide due to the presence of the Shillong plateau and Burmese range to the South. The Brahmaputra is steeper, more channelled and remains a braided river until its confluence with the Ganga. Ganga and Brahmaputra merge in Bangladesh to form the Lower Meghna that finally supplies the Indian Ocean in the Bay of Bengal.

Geologically, the Himalayan range is divided in four superimposed units (e.g. LE FORT, 1989). From North to South: the Tethyan Sedimentary Series consists of variably metamorphosed clastic sediments and carbonates, the High Himalaya Crystalline formations (HHC) are composed of orthogneisses, highly metamorphosed paragneisses and some marbles, the Lesser Himalaya (LH) is composed of metamorphosed metasediments, including minor black shales and limestones, finally, the Siwaliks forms the frontal range and is composed of sandstones and conglomerate that are uplifted Mio-Pliocene sediments deposited in the paleo-floodplain. To the south of the range, the floodplain is entirely composed of Quaternary fluvial sediment. Fluvial migration being intense most deposits are Holocene.

The G-B basin is one of the most densely populated of the world and the vegetation is consequently largely controlled by human activities (i.e. deforestation and farming). In the Himalayan range, the forest is still dominant although it has been severely affected by deforestation during the last decades. The vegetation distribution is however largely controlled by altitude and alpine scrub grassland dominate above 3000 to 3500 m

(DOBREMEZ, 1976). In the floodplain, the vegetation is composed of a mixture of crops and tropical grasslands. The main crops are rice, wheat, millet, maize and sugar cane. The contribution of C4 crops to the total production is variable but significant, reaching 80 % in the Uttar Pradesh state (AUCOUR et al., 2006).

To describe the G-B fluvial system, we sampled both Himalayan rivers at or near the outflow of the range and rivers in the floodplain (fig. 1). Most sampling was performed during the peak monsoon period (July-August, see Electronic Annex fig. 1). While there is seasonal variation in the sediment composition (e.g. AUCOUR et al., 2006), monsoon sampling is representative as 95% of the sediment transport occurs during this period (ISLAM and JAMAN, 2006). Suspended sediments were sampled at different depths in the river, from surface to bottom, in order to take into account sediment sorting. Bed sediments were dredged at the bottom of the rivers. This procedure was coupled with current velocity measurements with an Acoustic Doppler Current Profiler (ADCP) allowing the integration of the sediment variability over the whole river section. A few suspended and bank sediments were also collected either before or after the monsoon season.

In the Ganga basin, we sampled three of the major Trans-Himalayan tributaries of the Ganga at their outlet of the Himalaya in Nepal: the Karnali, the Kosi and the Narayani. The Kosi and the Narayani have also been thoroughly sampled before their confluence with the mainstream of the Ganga. In Nepal, we sampled large mountainous rivers of the Narayani basin (Kali Gandaki, Trisuli, Seti Kola) as well as secondary tributaries (Karnala, Rapti). The Gomati river, a pure plain river isolated from direct Himalayan supply (SINGH et al., 2005a), was used as an approach of the floodplain input. The mainstream of the Ganga was sampled in India at several stations along its course in the floodplain and finally sampling has been carried out in triplicate at Harding Bridge (Bangladesh) just before its confluence with the Brahmaputra. In

2005, the Narayani and Kosi in Nepal were also sampled using a depth profile but were not combined with ADCP.

A similar approach was applied for the Brahmaputra basin. We sampled major Trans-Himalayan tributaries (Siang, Subansiri, Manas and Tista) at the outlet of the Himalayan range or in the floodplain before their confluence with the Brahmaputra and the mainstream along its course in the floodplain (SINGH and FRANCE-LANORD, 2002). Finally, the sampling has been repeated over three monsoon seasons at Sirajganj (Bangladesh) before its confluence with the Ganga.

In order to estimate the contribution of fossil C_{org} derived from bedrock erosion, we analysed gravels extracted from bed sediments of several mountainous Himalayan rivers collected in Nepal and Arunachal Pradesh. These coarse sediments were sieved to eliminate the $< 2\text{mm}$ and $> 4\text{mm}$ fractions and the remaining gravels were rinsed with H_2O_2 (30% v) to eliminate any trace of C_{org} adsorbed to the surface of the gravels. Special care was also taken to eliminate any large debris of C_{org} . For each sample approximately 500 gravel particles corresponding to small fragments of bedrocks (see Electronic Annex fig. 2) are mixed together. Each gravel sample therefore represents an average sampling of the bedrock of the basin. The average TOC and Al/Si ratio obtained from the gravel samples are comparable to that calculated using a data base of individual rock samples (GALY et al., 2007b), showing that gravel samples are representative of source rock composition.

2.2 Organic carbon content and stable isotopic composition

The determination of total C_{org} content and stable isotopic composition in Himalayan river sediments is not straightforward as they contain significant amounts of detrital carbonates, including dolomite grains. Indeed, this requires the use of a liquid acid leaching

decarbonation that solubilizes significant amounts of C_{org} . Detailed description of this method as well as calibration data allowing the taking into account C_{org} solubilization during decarbonation are described in GALY et al. (2007a). Samples were crushed in an agate mortar and leached with 4 % HCl at 85 °C during 1 hour to remove any carbonate particles (including detrital dolomite). After careful rinsing and drying at 50 °C, samples were homogenised in an agate mortar. Elemental and isotopic compositions were then determined using a modified EuroEA3028-HT elemental analyser coupled to a GV Instruments IsoPrime continuous-flow isotope mass spectrometer. Total C_{org} concentrations (TOC^+) were then calculated from the C_{org} content determined on decarbonated sediments. The abbreviation TOC^+ indicates that total organic carbon measurements have been corrected for C_{org} loss during carbonate removal through liquid acidification, using the calibration presented in GALY et al. (2007a). EA-IRMS runs were calibrated using 2 lab standards with mineral matrix, C_{org} content and $\delta^{13}C_{org}$ comparable to those of the samples. TOC^+ was expressed in weight per cent of bulk sediment and $\delta^{13}C_{bulk}$ was expressed versus V-PDB using the δ notation (COPLIN, 1996). On the basis of repeated internal standards analysis and samples replicates, estimated overall reproducibility for TOC^+ and $\delta^{13}C_{org}$ is 0.03 % and 0.25 %, respectively.

2.3 Sediment analyses

Major and trace element concentrations were measured by ICP-AES and ICP-MS at Service d'Analyse des Roches et des Minéraux (CRPG-Nancy) on bulk sediment after lithium metaborate fusion. The typical analytical precision of major element concentration is better than 2%.

Grain size distributions were determined for selected samples using a laser diffraction analyser Malvern Mastersizer in the 1.2-600 μm size range. Representative aliquots were subsampled after bulk sediment drying at 50°C. Large aggregates formed during drying were gently broken in an agate mortar and further dispersed through controlled ultra-sonication. For selected sediments, we also directly measured grain size distribution on untreated wet sediments. Grain size distributions determined from dried and wet sediments were highly similar, suggesting that preliminary dispersion treatments of samples do not generate any significant artefacts. Results are volume based and are expressed as particle volume versus sphere diameter of equivalent volume. Although the size distributions may be slightly biased by sample treatment, they are reproducible by different methods (wet, dry), appear to be representative, and provide a consistent basis for comparison.

Nitrogen adsorption-desorption isotherms at 77 K were recorded with a step-by-step automatic lab-made setup. Samples were initially degassed at 50°C and 10^{-5} Pa for 18 hours. Adsorption-desorption isotherms were then determined by subjecting samples to various partial pressures of N_2 at 77 K. The specific area (SA) was calculated following the Brunauer Emmet Teller (BET) method (BRUNAUER et al., 1938). The proportion of micropores (diameter lower than 2 nm) was estimated following the t -plot method (DE BOER et al., 1966). Organic matter was not removed prior to N_2 sorption analyses since limited amounts of C_{org} in studied sediments must have resulted in negligible artefacts (MAYER, 1994). Maximum 2 s.d. uncertainty on specific area measurements is $\pm 0.25 \text{ m}^2\text{g}^{-1}$.

3. RESULTS

In large rivers of the G-B fluvial system sediment characteristics are highly variable with water depth (GALY et al., 2007b). This variation results from mineral and grain size sorting under hydrodynamic forces during transport. At the base of the range and in the floodplain

(fig. 1) we sampled suspended sediments along depth profiles in order to describe the whole sediment heterogeneity. The depth profile data are presented in Table 1.

The general G-B sediment characteristic is a relatively low C_{org} content (AUCOUR et al., 2006; GALY et al., 2007b; SUBRAMANIAN and ITTEKKOT, 1991). In bulk sediments, C_{org} content is generally lower than 1 % and has an arithmetic average value of ca. 0.35 %. Bed sediments dredged from the bottom of the river have systematically lower C_{org} content than suspended sediments with an average value lower than 0.1 %. Direct observation shows that organic matter is different in bottom and upper suspended sediments (fig. 2). Bottom and coarse-grained sediment, almost systematically contain macroscopic vegetal debris that are more or less decomposed. Such debris is absent in upper (fine-grained) sediments in spite of the presence of plant raft floating at the surface. In upper sediments, transmitted electron microscope (TEM) observations on resin-embedded samples reveal that microscopic C_{org} fragments are present aggregated to mineral particles as well as independent particles.

3.1 Relation between C_{org} content and Al/Si

Details of the major relationships described in this study (best fit parameters and statistical relevance) are listed in the Electronic Annex Table 1.

The whole set of sediment samples from large rivers (mountainous and floodplain rivers) defines a clear positive correlation between TOC^+ and Al/Si (mol:mol), as previously observed for Ganga, Brahmaputra and Lower Meghna sediments in Bangladesh (GALY et al., 2007b). This relationship allows comparison of the C_{org} loading (i.e. the TOC^+ for a constant Al/Si ratio) of different rivers or sampling sites.

3.1.1 Ganga basin

Reported in a TOC^+ versus Al/Si diagram, sediments from Himalayan rivers, floodplain rivers as well as Ganga define positive linear correlations (fig. 3). Each sampling site defines an individual trend but the overall variability in their slope is limited and they tend to converge towards similar TOC^+ value ($< 0.05\%$) for low Al/Si ratios. Among the Large Trans-Himalayan tributaries, Narayani and Kosi have very comparable C_{org} loading. The Karnali seems to have significantly higher loading (based on a single suspended sediment). Large tributaries of the Narayani sampled in the Himalayan range have comparable C_{org} loading to the Narayani at the outflow of the Himalaya. Detailed depth sampling on the Ganga river at different locations from Varanasi downstream to Harding Bridge also define distinct trends showing that C_{org} loading is not absolutely constant throughout the river course. Nevertheless, samples collected during three different monsoons at Harding Bridge define highly similar trends suggesting a rather constant C_{org} loading at the outflow of the basin.

3.1.2 Brahmaputra basin

The Brahmaputra at Sirajganj was sampled in detail four times during the 2002, 2004 and 2005 monsoons. The four sets of samples define a unique trend in the TOC^+ versus Al/Si diagram indicating constant C_{org} loading (fig. 4). Sediments from the Brahmaputra mainstream sampled along its course in the plain are consistent and have comparable or slightly higher C_{org} loading than the Brahmaputra at Sirajganj. Sediments of the four Trans-Himalayan tributaries of the Brahmaputra define distinct trends in the TOC^+ versus Al/Si diagram. The Siang and the Tista rivers have comparable C_{org} loading, slightly lower than that of the mainstream. Sediments from the Subansiri and the Manas have higher C_{org} loading than mainstream sediments. Secondary Himalayan tributaries are all very distinct from the Transhimalayan tributaries and the mainstream with C_{org} loading 4 to 5 times higher.

3.2 Grain size

In the Shepard's diagram (not shown), river sediments from the G-B system can be classified as silt, silty sand, sandy silt and sand. Bed sediments are coarser than suspended sediments and fall in the range of pure sand. Surface suspended sediments are the finest and fall in the range of pure silt. The proportion of clay ($< 2 \mu\text{m}$) is always limited and reaches a maximum of ca. 10 % in surface suspended sediments. Bed and surface suspended sediments generally have uni-modal grain size distribution whose respective mode is $> 100 \mu\text{m}$ and $< 50 \mu\text{m}$. Suspended sediments at intermediate depth have bi-modal distributions realising a continuum between the surface suspended sediment and the bed sediment (fig. 5). For the whole set of sediment, TOC^+ is correlated with the proportion of fine particles. The data are best modelled by a power curve, although the deviation from linearity is small. The proportion of $< 25 \mu\text{m}$ particles gives the best correlation between TOC^+ and grain size (fig. 6). Sediments from the Brahmaputra and the Ganga in Bangladesh define distinct trends. For a given proportion of fine particles, Brahmaputra sediments have slightly higher TOC^+ than Ganga sediments. In such a diagram, suspended sediments from the Kosi and Narayani river are comparable with suspended sediments from the Ganga in Bangladesh. However, suspended sediment from the Karnali as well as Ganga sediments sampled in the Indian floodplain (Patna) have slightly higher relative C_{org} content and appear to be more comparable with sediments from the Brahmaputra.

3.3 Sediment load

During the monsoon, G-B rivers have high total suspended sediment concentration (TSS). There is however a large variability from 0.3 to 10.2 g/l. TSS are generally higher at the base of the range than in the floodplain, mostly related to more turbulent and powerful flow. Depth

sampling profiles show a quasi-linear increase of TSS with depth ((GALY et al., 2007b), table 1), both at the base of the range and in the floodplain. For instance, in the Narayani at the base of the range, TSS increase from 2.9 g/l at the surface to 10.2 g/l near the bottom. This illustrates the large sorting process affecting the sediments during fluvial transport.

C_{org} content of suspended sediments generally decreases with increasing TSS. In a $1/TOC^+$ versus TSS diagram, sediments from the Ganga and Brahmaputra basins define similar positive trends characterized by higher scatter for high TSS values (Electronic Annex fig. 3). The intercept of these trends when TSS tends to 0 is greater than 0.01, indicating that these relationships are not attributable to pure dilution effects (see EA).

3.4 Specific area

BET specific area has been measured for selected samples of the Ganga and Brahmaputra in Bangladesh. Specific areas range between 1.3 and 34.8 m^2g^{-1} . Bed sediments from the Ganga and the Brahmaputra have very low values, respectively 1.3 and 1.8 m^2g^{-1} . Suspended sediments have higher specific area, ranging between 3.6 and 8.9 m^2g^{-1} for Brahmaputra suspended sediments and between 17.4 and 34.3 m^2g^{-1} for Ganga suspended sediments. This is consistent with the mineralogy of the clay fraction in these rivers since Ganga sediments carry more than 50 % of smectite whereas Brahmaputra sediments have clays dominated by illite with negligible proportion of smectite (HEROY et al., 2003). Ganga and Brahmaputra sediments present very different N_2 adsorption-desorption isotherms revealing contrasting pore size distributions (fig. 7). We determined the proportions of micropores (< 2 nm) using the t -plot method. Brahmaputra sediments have a negligible proportion of micropores, whereas they represent 19 to 25 % of the total surface area in Ganga sediments. Specific area

corrected for the surface associated to micropores represents the external specific area. Ganga suspended sediments have external specific areas ranging from 13.7 to 26.0 m²g⁻¹, i.e. still significantly higher than that of Brahmaputra suspended sediments. TOC⁺ and specific area are well correlated but Ganga and Brahmaputra sediments define very distinct trends (fig. 8). Brahmaputra and Ganga suspended sediments have respective TOC⁺/SA ratios of 0.73 ± 0.02 and 0.20 ± 0.01 mgCg⁻¹. For Ganga suspended sediments this ratio increases to 0.23 ± 0.02 mgCg⁻¹ when calculated using external specific area.

3.5 Stable C isotopic composition

3.5.1 Ganga basin

Sediments from the Kosi, Narayani and Karnali rivers at the outlet of the Himalaya have $\delta^{13}\text{C}_{\text{org}}$ values between -23.6 and -25.6 ‰. $\delta^{13}\text{C}_{\text{org}}$ of bed sediments is higher than that of suspended sediments which are comparatively enriched in C_{org}. In suspended sediments, $\delta^{13}\text{C}_{\text{org}}$ value decreases with C_{org} content and for the Kosi and the Narayani the surface suspended sediment is the most ¹³C depleted (fig. 9). Suspended sediments of the Kosi and Karnali rivers have $\delta^{13}\text{C}_{\text{org}}$ values ca. 1 ‰ lower than suspended sediments of the Narayani river. Suspended sediments of large mountainous rivers of the Narayani basin have variable $\delta^{13}\text{C}_{\text{org}}$ value from -25.0 to -22.4 ‰. However, their average $\delta^{13}\text{C}_{\text{org}}$ value (-24.3 ‰) is comparable to that of the Narayani at the outflow of the Himalaya. Suspended sediments from the Kosi and the Gandak (name of the Narayani in India) sampled before their confluence with the mainstream of the Ganga have higher $\delta^{13}\text{C}_{\text{org}}$ values (ca. 2 ‰) than at the outlet of the Himalaya. Secondary Himalayan tributaries have $\delta^{13}\text{C}_{\text{org}}$ values from -24.4 to -25.6 ‰, comparable to that of Trans-Himalayan rivers. Suspended sediments from Ganga mainstream have higher $\delta^{13}\text{C}_{\text{org}}$ than bed sediments. On the contrary to Himalayan tributaries, $\delta^{13}\text{C}_{\text{org}}$ of

suspended sediments increases with TOC^+ . Suspended sediments from different locations along the mainstream of the Ganga in the Indian floodplain have variable $\delta^{13}\text{C}_{\text{org}}$ with average values ranging from -21.2 ‰ at Varanasi to -22.3 ‰ at Manihari. The three detailed depth samplings realised at Harding Bridge during the 2002, 2004 and 2005 monsoons show noticeable $\delta^{13}\text{C}_{\text{org}}$ differences from one monsoon to another. The average $\delta^{13}\text{C}_{\text{org}}$ of suspended sediments varies from -22.2 ‰ in 2002 to -20.7 ‰ in 2005. Suspended sediments sampled at Harding Bridge therefore have systematically higher $\delta^{13}\text{C}_{\text{org}}$ values than suspended sediments sampled at the outlet of the Himalaya. Bed sediments dredged at the bottom of the river at Harding Bridge have lower $\delta^{13}\text{C}_{\text{org}}$ than their corresponding suspended sediments with an average value of -22.5 ‰. Two suspended sediments sampled at Patna during the dry season (May) have very low $\delta^{13}\text{C}_{\text{org}}$ value compared to Ganga suspended sediments sampled during the monsoon; their average value is -26.3 ‰. The total sediment concentration that was 5 to 10 times lower than during the monsoon, as well as the presence of abundant algae in the surface water, indicate that these low $\delta^{13}\text{C}_{\text{org}}$ values derive from a greater contribution of autochthonous organic matter.

3.5.2 Brahmaputra basin

In every river of the Brahmaputra basin, bed sediments have higher $\delta^{13}\text{C}_{\text{org}}$ values than suspended sediments. The $\delta^{13}\text{C}_{\text{org}}$ of suspended sediments tends to decrease with increasing C_{org} content and surface suspended sediments generally have the lowest $\delta^{13}\text{C}_{\text{org}}$ value (fig. 10). Bed sediments from Trans-Himalayan rivers have variable $\delta^{13}\text{C}_{\text{org}}$ values between -19.9 ‰ and -23.7 ‰ with an average value of -22.1 ‰. Suspended sediments from the same rivers also have variable $\delta^{13}\text{C}_{\text{org}}$ values between -23.7 ‰ and -26.3 ‰ with an average value of -24.8 ‰. Sediments from secondary Himalayan tributaries tend to have slightly higher $\delta^{13}\text{C}_{\text{org}}$, with an average value of -24.0 ‰ for suspended sediments. Suspended sediments from the

Brahmaputra mainstream sampled during the monsoon at different locations in the Indian plain have quite comparable $\delta^{13}\text{C}_{\text{org}}$ with an average value of -23.7‰ . The four detailed depth sampling realised at Sirajganj during the 2002, 2004 and 2005 monsoons show minor $\delta^{13}\text{C}_{\text{org}}$ differences. The average $\delta^{13}\text{C}_{\text{org}}$ value of suspended sediments varies between -22.9‰ and -23.8‰ . The 0.9‰ difference between the two detailed samplings performed in July 2004 shows that the composition of suspended sediments may be subject to rapid temporal variations within a week. Suspended sediments from the Brahmaputra at Guwahati (India) sampled at the end of October, i.e. after the monsoon season, have significantly lower $\delta^{13}\text{C}_{\text{org}}$ than suspended sediments sampled during the monsoon, with an average value of -24.9‰ . This likely derives from a greater contribution of autochthonous organic matter, as documented for the Ganga during the dry season before the monsoon.

3.5.3 $\delta^{13}\text{C}_{\text{org}}$ of source rock fossil C_{org}

The gravel sampling allows integration of a considerable number of lithologies over large sub-basins, and provides a good estimate of the average fossil C_{org} eroded from the source rocks and transferred to the river sediments. Gravels from the bed of Himalayan mountainous rivers have highly variable $\delta^{13}\text{C}_{\text{org}}$ between -28.0 and -14.6‰ (table 2). There is no systematic difference between gravels from rivers draining the two main lithologic units, the High Himalaya Crystalline (HHC) and the Lesser Himalaya (LH), as both have variable $\delta^{13}\text{C}_{\text{org}}$. The average $\delta^{13}\text{C}_{\text{org}}$ value calculated for the whole set of gravel samples is -22.6‰ but the dispersion of the data is quite high (-28.0 to -14.6‰).

4. DISCUSSION

4.1 Sedimentological control of C_{org} loading

The amount of C_{org} exported by rivers results from a complex interaction between organic matter produced and decomposed within the basin and mineral particles derived from rock erosion. Physical and chemical properties of sediment must therefore exert a control on the C_{org} loading of sediments. Three sediment properties have been identified as the main factors that determine C_{org} loading in detrital sediments (e.g. Mayer, 1994; Sollins et al., 1996; Ransom et al., 1998): (1) the specific area of mineral particles (2) the particle size, especially the proportion of fine particles and (3) the mineralogy. However, in spite of several studies, the respective part of each parameter in the control of C_{org} loading remains unclear. In addition, each river system is characterised by different source rocks, physical and chemical erosion rates or transport dynamics that must result in different C_{org} loading mechanisms. Earlier studies have proposed that specific area exerts a dominant control on C_{org} loading in river sediments by C_{org} adsorption to mineral surfaces (e.g. HEDGES and KEIL, 1995; MAYER, 1994). This hypothesis has mainly been inspired and supported by the single positive correlation between TOC^+ and specific area found for different river systems (e.g. KEIL et al., 1997). It assumes that a single layer of C_{org} covers the entire mineral surface. This monolayer equivalent model was initially used to explain the control of C_{org} loading by specific area as it yields a TOC^+/SA ratio compatible with that observed by the authors (0.6 to 1.5 mgC/m²). Nevertheless, progress in surface analyses as well as new observation techniques showed that the monolayer equivalent theory is not adequate since only a minor proportion (ca. 15%) of the mineral surface is effectively covered by C_{org} (BOCK and MAYER, 2000; MAYER, 1999). In addition, several studies have shown that C_{org} is not linked to mineral surface as a single adsorbed layer but rather forms patchy organo-mineral aggregates similar to those observed in this study (fig. 2) (e.g. CURRY et al., 2007; FURUKAWA, 2000; WAGAI and MAYER, 2007).

440 The comparison between Ganga and Brahmaputra sediments provides an insightful case study to address the role of specific area on C_{org} loading in river sediments because both rivers have quite comparable physiographic, geologic and vegetation characteristics but contrasted sediment specific areas. As mentioned in section 3.4, this difference in specific surface areas is only due to the clay composition with high proportion of smectite for the Ganga compared to Brahmaputra. This leads to specific areas of Ganga sediments that are 4 to 5 times higher than those of Brahmaputra sediments for comparable TOC^+ , grain size or Al/Si ratio. Brahmaputra suspended sediments have OC/SA ratio in the range defined as "typical river sediment OC/SA ratio" whereas Ganga suspended sediments have lower OC/SA that fall in the range defined as "typical deltaic sediment OC/SA ratio" (e.g. HEDGES and OADES, 1997).

450 This implies that SA does not exert a first order control on C_{org} loading, i.e. that C_{org} loading of river sediments is primarily determined by other intrinsic or extrinsic parameters, such as mineralogy, grain size or primary productivity in the basin. Rather the clear relationship between TOC^+ and SA (fig. 8) results from the co-variation of specific area with other sedimentological characteristics (Electronic Annex fig. 4). Moreover, the SA of river sediments appears to be controlled by minor mineral phases that have very high SA, such as smectite. OC/SA ratio is therefore not a good proxy to compare C_{org} loadings in different rivers. This is further supported by the Huanghe river sediments that have low OC/SA ratio, comparable to that of Ganga suspended sediments (KEIL et al., 1997), mainly because their clay fraction has significant proportion of smectite (PARK and KHIM, 1992).

460 In river sediments, grain size and mineralogy are generally not independent parameters; e.g. clays and sand are differentiated by their particle size but also have very different mineral compositions. This makes it difficult to decouple the parameters controlling C_{org} loading. Correlations between C_{org} content and the proportion of fine particles have classically been reported in river sediments (e.g. KEIL et al., 1997). Positive co-variation between C_{org} content

and the proportion of fine particles may result from at least two factors depending on how C_{org} is transported: (1) if C_{org} is mainly independent of minerals particles, its low density would tend to concentrate C_{org} in fine-grained sediments through hydrodynamic sorting, (2) if C_{org} is mainly linked with minerals, both particle size and mineral composition must control the C_{org} loading in detrital sediments. In this case, C_{org} is associated with particles as organo-mineral complexes (WAGAI and MAYER, 2007), or can be encapsulated within particle microfabrics (CURRY et al., 2007), and are preferentially associated with particle edges (FURUKAWA, 2000; MAYER et al., 2004). Therefore, multiple physical parameters such as particle charge density, chemical composition (nature of exchangeable cation), crystalline structure, size and shape must all determine the ability of C_{org} to be bonded with particles (SOLLINS et al., 1996).

In the G-B river system, the chemical composition of bed and suspended sediments can be explained by mineralogical mixing. In an Fe/Si versus Al/Si diagram, river sediments define a mixing line between a quartz rich end-member and a phyllosilicate rich end-member (GALY and FRANCE-LANORD, 2001; SINGH and FRANCE-LANORD, 2002). Bed and suspended sediments are differentiated by the combined effect of shape, density and grain size segregation that control the flotation properties of particles. This tends to concentrate coarse and rounded minerals (quartz, feldspars) towards the bottom and fine grained and flaky particles (micas, clays) towards the surface. Since quartz and phyllosilicates represent more than 80% of the silicates, the Al/Si ratio is a function of the relative proportions of quartz and micas+clays and allows representation and quantification of this hydrodynamic differentiation process. For the whole set of river sediment, there is a general co-variation between Al/Si ratio and grain size parameters such as the proportion of $<25 \mu\text{m}$ particles (Electronic Annex fig. 5). The general positive correlation between TOC^+ and Al/Si therefore indicates that C_{org} content also responds to hydrodynamic segregation processes: (1) organic particles tend to concentrate in surface waters because of their low density and fibrous shapes, and (2) organo-

mineral aggregates are preferentially formed from clays and to a minor extent from micas and therefore tend also to concentrate in surface regions.

4.2 C_{org} loading evolution along the G-B river system

Since sediment characteristics exert a primary control on C_{org} content, comparing C_{org} loading at different locations in the basin requires a common reference. Al/Si ratios are probably the best reference as they clearly allow taking into account the combined sedimentological effects. At the basin scale, this ratio is not necessarily conservative with respect to weathering, however in the Himalayan case the chemical erosion of Si represents less than 1% of its solid flux (GALY and FRANCE-LANORD, 1999) and Al/Si ratios are essentially insensitive to weathering processes. Therefore we use the slope defined by sediments from a given location in the Al/Si ratio vs. TOC^+ diagram to compare the C_{org} loading of sediments independently of mineralogy, specific area or grain size distribution.

C_{org} loading of suspended sediments from the Ganga and Brahmaputra in Bangladesh are highly comparable and stable over the three monsoon samplings studied. This likely derives from the relative stability of sediment composition throughout time and reflects the buffering effect of such a large river system. The different Trans-Himalayan tributaries have either slightly higher or slightly lower C_{org} loading than Ganga and Brahmaputra in Bangladesh. Our sampling may not be fully representative, as most of these large rivers have been sampled only once. However, the Narayani and the Kosi have been sampled twice and detailed depth sampling has been performed on these rivers. Our results indicate similar C_{org} loading for the two samplings, supporting the representativeness of our data. Secondary Himalayan tributaries of the Brahmaputra have systematically higher C_{org} loading than Trans-Himalayan tributaries. C_{org} loading differences between Himalayan rivers may be related to differences in

physical erosion characteristics such as the respective proportions of sediment generated by glacier and landslides or overall physical erosion rates. More data within the mountain basins would be required to support this inference as precise comparison of contrasting Himalayan basins would certainly provide insightful constraints on the control of C_{org} loading in river sediments.

520 In the Brahmaputra basin, the Trans-Himalayan tributaries which represent the large majority of the sediment influx to the floodplain have higher or lower C_{org} loading than the Brahmaputra in Bangladesh and different samplings along the Brahmaputra course do not show any simple evolution of the C_{org} loading. As a consequence, we can reasonably estimate that average C_{org} loading at the outflow of the Himalayan range must be quite comparable to that in Bangladesh.

The Ganga sampled in the Indian floodplain at Varanasi and Patna has higher C_{org} loading than further downstream in Bangladesh. The influx of sediments to the Ganga from the Narayani-Gandak and Kosi which have lower C_{org} loading explains this evolution. For the Kosi and the Narayani-Gandak, there is no evolution of the C_{org} loading from Himalaya to
530 their confluence with the Ganga (Electronic Annex fig. 6). The contrast of loading between western and eastern Ganga floodplain is difficult to interpret in the absence of data for the upper Ganga and Yamuna. It may derive from a higher loading of western Himalayan tributaries as suggested by data of the Karnali-Gahgara; alternatively it may be due to organic matter addition in the floodplain. In any case, the higher loading of the western Ganga could result from an overall lower sediment yield of the west compared to the east (e.g. SINHA et al., 2005) as lower physical erosion should favour higher fixation of organic matter.

4.3 $\delta^{13}C_{org}$ of G-B river system: implication for the source and fate of C_{org}

540 4.3.1 Sources of C_{org}

In river sediments, $\delta^{13}C_{org}$ is determined by the relative contribution of different types of C_{org} such as higher plants, fossil C_{org} and phytoplankton. There is a strong isotopic contrast between the 2 major photosynthetic pathways that allows differentiation of C3 and C4 plant inputs in river sediments; C3 plants $\delta^{13}C_{org}$ ranges between -35 and -20 ‰ with an average value of -26 ‰ while C4 plants $\delta^{13}C_{org}$ ranges between -16 and -10 ‰ with an average value of -13 ‰ (DEINES, 1980). The freshwater phytoplanktonic matter usually has low $\delta^{13}C_{org}$. The isotopic fractionation between phytoplankton and dissolved inorganic carbon (DIC) has been estimated to be ca. -23‰ (MOOK and TAN, 1991). In the G-B rivers at the outflow of the range and in the floodplain, the $\delta^{13}C$ of DIC is between -8 and -12 ‰ during the monsoon (GAJUREL et al., 2006; GALY and FRANCE-LANORD, 1999; SINGH et al., 2005b). Phytoplanktonic organic matter must therefore have $\delta^{13}C_{org}$ values between -31 and -35 ‰. This is further supported by the $\delta^{13}C_{org}$ value (-32.1‰) measured by AUCOUR et al. (2006) in a low stage sediment of the Brahmaputra presenting a strong C_{org} enrichment (7.6%) and an obvious contribution of phytoplankton.

Fossil C_{org} contained in Himalayan source rocks has variable $\delta^{13}C_{org}$ between -31 and -18 ‰ (AUCOUR et al., 2006). Our data from gravel samples are consistent with individual source rock analyses, however, the average value calculated using source rock individual analyses (-25.5 ‰) is lower than that of gravels (-22.5 ‰). Because $\delta^{13}C_{org}$ values in source rocks are variable and overlap with recent C_{org} isotopic signatures, $\delta^{13}C_{org}$ values in river sediments are not diagnostic to estimate fossil C_{org} proportions. Using $\Delta^{14}C$ values of river sediments and the mean C_{org} content of Himalayan source rocks (0.05 to 0.08%), the proportion of fossil C_{org} has been estimated in Ganga, Brahmaputra and Lower Meghna sediments in Bangladesh (GALY et al., 2007b). The average proportion of fossil C_{org} has been conservatively estimated between 40 to 100 % in bed sediments and around 10-20 % in average suspended sediment.

For each river, suspended sediments have either higher or lower $\delta^{13}\text{C}_{\text{org}}$ values than bed sediments. In a TOC^+ vs. $\delta^{13}\text{C}_{\text{org}}$ diagram, they define mixing trends between a bed sediment endmember with low TOC^+ and $\delta^{13}\text{C}_{\text{org}} \approx -23\text{‰}$ and surface suspended sediment with higher TOC^+ and $\delta^{13}\text{C}_{\text{org}}$ around -20 to -22‰ for the Ganga or -24 to -26‰ for other rivers (figs. 9 and 10). We interpret these trends as a mixing between bed sediment dominated by fossil C_{org} and surface suspended sediment dominated by recent biogenic C_{org} such as soil organic matter or fresh plant debris. The recent organic matter is however markedly different for the Ganga than for other rivers either in Himalaya or on the Brahmaputra side. In Trans-Himalayan and secondary Himalayan tributaries of the Ganga and Brahmaputra basins, the $\delta^{13}\text{C}_{\text{org}}$ values of suspended sediments around -25 ‰ indicate a contribution of recent C_{org} dominated by C3 plants. This is consistent with Himalayan vegetation that is largely dominated by C3 species (BLASCO et al., 1996; DOBREMEZ, 1976; GALY et al., Submitted). The contribution of phytoplanktonic organic matter appears to be limited since its $\delta^{13}\text{C}$ is very low (-31 to -35 ‰) i.e. significantly lower than that of C3 plants. This minimal contribution is consistent with the high turbidity and current velocity of such mountainous rivers during the monsoon season.

Suspended sediments of the Ganga and Brahmaputra in the plain define opposite mixing trends as surface suspended sediments have respectively higher and lower $\delta^{13}\text{C}_{\text{org}}$ than bed sediments. This reveals different recent C_{org} sources. While suspended sediments of the Brahmaputra have similar $\delta^{13}\text{C}_{\text{org}}$ values to that of its Trans-Himalayan tributaries, suspended sediments of the Ganga in the plain have $\delta^{13}\text{C}_{\text{org}}$ values that are on average 2 to 4 ‰ higher than that of its Himalayan tributaries.

4.3.2 fate of C_{org} in the Ganga basin

The evolution of $\delta^{13}\text{C}_{\text{org}}$ from Himalaya to the Ganga shows that organic matter with a significant proportion of C4 plant is incorporated into the river sediment during the floodplain

transit (fig. 11). This is consistent with the presence of natural C4 grasses and cultivated C4 crops in the floodplain (AUCOUR et al., 2006 and ref. therein). Such evolution implies either an addition of C_{org} during transit or a replacement. In the Kosi and Narayani rivers, the $\delta^{13}C_{org}$ values of the suspended sediments increase of ca. 2 ‰ from the Himalayan range to the confluence with the Ganga (fig. 11) without increase of their C_{org} loading (Electronic Annex fig. 6). The Gomati river, which is a pure plain river isolated from direct Himalayan supply for several thousand years (SINGH et al., 2005a), can be used as an analogue of the plain C_{org} input. While it was sampled only once and may not be representative of the whole Gangetic plain, its $\delta^{13}C_{org}$ value (-21.9‰) suggests that floodplain C_{org} input is composed of mixed C4 and C3 plants. This suggests that average floodplain organic matter is not significantly different from that of the Ganga suspended sediment and it rules out the hypothesis of a simple addition of pure C4 organic matter during the plain transit.

The alternative is therefore that part of the C_{org} derived from mountainous vegetation is oxidised and replaced by C_{org} derived from the plain vegetation. This C_{org} renewal process likely occurs during the repeated deposition-erosion cycles affecting the sediments from one monsoon to the other as well as during river course avulsion. Estimating the proportion of renewed C_{org} is not straightforward as we do not precisely know the composition of the plain C_{org} . Nevertheless, taking into account estimates of the cultivated areas covered by C3 and C4 plants in the plain (AUCOUR et al., 2006), and the composition of the Gomati river we can propose that a minimum of 50 % of the C_{org} is renewed. The $\delta^{13}C_{org}$ variability between suspended sediments of the Ganga in Bangladesh sampled in 2002, 2004 and 2005 may either reflect a variation of the proportion of C_{org} that is renewed or a variation of the composition of the plain input. The relative stability of the bed sediments $\delta^{13}C_{org}$ value as well as the fact that mixing trends defined by Ganga suspended sediments are opposed to that defined by Himalayan rivers suspended sediments indicate a selective preservation of the rock derived

fossil C_{org} . This is consistent with its highly refractory character that makes it very resistant to oxidation (e.g. BLAIR et al., 2003).

4.3.2 fate of C_{org} in the Brahmaputra basin

In the Brahmaputra basin, in contrast to the Ganga basin, there is no clear $\delta^{13}C_{org}$ change from the outlet of the Himalaya to the delta (fig. 13). This may indicate that there is no C_{org} renewal during the fluvial transport from the outflow of the Himalayan range to the delta or that there is no C3/C4 contrast between the Brahmaputra floodplain and the Himalaya. The Brahmaputra plain is almost exclusively cultivated with C3 crops (AUCOUR et al., 2006) and the proportion of C4 plants in its natural vegetation should be lower than in the Gangetic plain due to more humid conditions. The average $\delta^{13}C_{org}$ of Brahmaputra plain vegetation may thus be very close to that of its Himalayan tributaries. This is further supported by vegetation simulations obtained using the Dynamic Vegetation Model CARAIB (GALY et al., Submitted). Consequently, any renewal of C_{org} during the Brahmaputra transit would have only minor effect on $\delta^{13}C_{org}$ of river sediments. Consequently, more specific tracers are required to precise the fate of C_{org} in the Brahmaputra basin. However, the characteristics of the two rivers and their respective floodplains are different: the Ganga is a meandering river with a large floodplain whereas the Brahmaputra is a braided river with a narrow floodplain. The residence time of river sediments is a key parameter controlling the extent of C_{org} oxidation during fluvial transport (e.g. AUFDENKAMPE et al., 2007; BLAIR et al., 2004). The morphological and hydrodynamic differences between Ganga and Brahmaputra rivers could therefore favour a longer transit, hence a more efficient renewal in the Ganga than in the Brahmaputra.

5. CONCLUSIONS

The comparison between Ganga and Brahmaputra sediments that have comparable C_{org} content but highly different specific area clearly indicates that specific area is not the key parameter that determines C_{org} content in such sediments. In G-B fluvial sediments, C_{org} is both present as independent particles and intimately linked to mineral particles. The control of C_{org} loading in these sediments appears to be related to: (1) organic particles segregation under hydrodynamic forces in the river and, (2) the ability of mineral particles to form aggregates in which C_{org} can be encapsulated. As a consequence, sorting processes generated by fluvial transport, which mainly determine sediment characteristics, exert a first order control on C_{org} loading in G-B river sediments. Estimation of C_{org} loading in river sediments is therefore highly sensitive to the representativeness of the sample set that is used. The depth profile sampling procedure applied to G-B rivers allows the sediment heterogeneity in the river to be taken into account. This sampling provides a range of sediment compositions naturally generated by sorting processes during the fluvial transport. The comparison of TOC^+ to a conservative parameter describing the bulk sediment characteristics, such as Al/Si , therefore allows the actual C_{org} loading in sediments exported by the river to be characterised. During the monsoon, C_{org} loading appear to be rather constant from large trans-Himalayan rivers sampled at the base of the range to Ganga and Brahmaputra sampled in the Bangladeshi delta. At the base of the Himalayan range, $\delta^{13}C$ of bulk organic matter reveals a mixing between C_3 plant inputs and fossil C_{org} derived from source rock erosion. In the delta, organic matter transported by the Brahmaputra results from similar mixing while organic matter transported by the Ganga clearly results from the mixing between fossil C_{org} and a C_4 plant rich end-member mainly originating from the floodplain. During the Gangetic floodplain transit, recent C_{org} derived from the Himalaya is oxidised and is replaced by C_{org} derived from the

floodplain. This process is likely related to channel avulsion, generating re-erosion of sediments previously deposited in the plain. Determining the extent of such a renewal process would require knowing the exact $\delta^{13}\text{C}$ of the floodplain C_{org} . However, conservative hypotheses indicate that at least 50 % of the C_{org} is renewed. The case of the Brahmaputra is ambiguous due to the lack of marked C3/C4 difference between Himalayan and plain vegetation. Differences in the floodplain width and rivers morphology however suggest lower C_{org} renewal rate for the Brahmaputra than for the Ganga. More focused tracers such as molecular level $\delta^{13}\text{C}$, δD and $\Delta^{14}\text{C}$ (e.g. DRENZEK et al., 2007; EGLINTON et al., 1996; SAUER et al., 2001) must have a great potential to track and quantify C_{org} renewal during fluvial transport. The study of the G-B fluvial system shows that processes associated with physical erosion and sediment transport exert a primary control on both loading and fate of riverine C_{org} . In addition, floodplains appear to play a determinant role in the terrestrial C_{org} dynamic acting as a "reactor" promoting both C_{org} oxidation and loading. Our study also indicates that large rivers may preferentially export terrestrial C_{org} produced in particular zones of the basin, such as floodplains. This process must be carefully addressed in the scope of paleo-vegetation and paleo-climate reconstructions based on riverine C_{org} buried in oceanic sediments. Finally, precise characterisation at the basin scale of both the terrestrial C_{org} dynamic and the relationships between physical erosion and C_{org} export should significantly improve models of the global C cycle.

Acknowledgements

This study was funded by CNRS-INSU programs "Eclipse" and "Relief de la Terre". We thank Prof. Mustafizur Rahman from Dhaka University, Dr Sunil K. Singh from PRL Amadabad, and Dr. Ananta Gajurel from Tribhuvan University for their constant

690 collaboration and help on the field. Angelina Razafitianamaharavo performed Nitrogen
adsorption-desorption experiments and is greatly thanked for her help in data treatment.
Caroline Guilmette is also acknowledged for her valuable help in the stable isotope
laboratory. Finally we thank Shuh-Ji Kao, two anonymous reviewers as well as Robert Aller
for their constructive remarks. This is CRPG contribution # XXXX.

REFERENCES

- Aucour, A.-M., France-Lanord, C., Pedoja, K., Pierson-Wickmann, A.-C., and Sheppard, S. M. F., 2006. Fluxes and sources of particulate organic carbon in the Ganga-Brahmaputra river system. *Global Biogeochemical Cycles* 20, 1-12. [10.1029/2004GB002324](https://doi.org/10.1029/2004GB002324)
- Aufdenkampe, A. K., Mayorga, E., Hedges, J. I., Llerena, C., Quay, P. D., Gudeman, J., Krusche, A. V., and Richey, J. E., 2007. Organic matter in the Peruvian headwaters of the Amazon: Compositional evolution from the Andes to the lowland Amazon mainstem. *Organic Geochemistry* 38, 337-364.
- Blair, N. E., Leithold, E. L., and Aller, R. C., 2004. From bedrock to burial: the evolution of particulate organic carbon across coupled watershed-continental margin systems. *Marine Chemistry* 92, 141-156.
- Blair, N. E., Leithold, E. L., Ford, S. T., Peeler, K. A., Holmes, J. C., and Perkey, D. W., 2003. The persistence of memory: the fate of ancient sedimentary organic carbon in a modern sedimentary system. *Geochimica et Cosmochimica Acta* 67, 63-73.
- Blasco, F., Bellan, M. F., and Aizpuru, M., 1996. A vegetation map of tropical continental Asia at scale 1.5 million. *Journal of Vegetation Science* 7, 623-634.
- Bock, M. J. and Mayer, L. M., 2000. Mesodensity organo-clay associations in a near-shore sediment. *Marine Geology* 163, 65-75.
- Brunauer, S., Emmet, P. H., and Teller, E., 1938. Adsorption of gases in multimolecular layers. *Journal of the American Chemical Society* 60, 309-319.
- Burdige, D. J., 2005. Burial of terrestrial organic matter in marine sediments: A reassessment. *Global Biogeochemical Cycles* 19. [10.1029/2004GB002368](https://doi.org/10.1029/2004GB002368)
- Coplen, T. B., 1996. New guidelines for reporting stable hydrogen, carbon, and oxygen isotope-ratio data. *Geochimica et Cosmochimica Acta* 60, 3359-3360.
- Curry, K. J., Bennett, R. H., Mayer, L. M., Curry, A., Abril, M., Biesiot, P. M., and Hulbert, M. H., 2007. Direct visualization of clay microfabric signatures driving organic matter preservation in fine-grained sediment. *Geochimica et Cosmochimica Acta* 71, 1709-1720.
- De Boer, J. H., Lippens, B. C., Linsen, B. G., Brokhoff, J. C. P., Van der Heuvel, A., and Osinga, T. J., 1966. The *t*-curve of multimolecular N₂ adsorption. *Journal of Colloid and Interface Science* 23, 577-599.
- Deines, P., 1980. The isotopic composition of reduced organic carbon. In: Fritz, P. and Fontes, J. C. Eds.), *Handbook of Environmental Isotope Geochemistry*. Elsevier, New York.

Dobremez, J. F., 1976. *Le Népal : écologie et biogéographie*, Paris.

Drenzek, N. J., Montlucon, D. B., Yunker, M. B., Macdonald, R. W., and Eglinton, T. I., 2007. Constraints on the origin of sedimentary organic carbon in the Beaufort Sea from coupled molecular ^{13}C and ^{14}C measurements. *Marine Chemistry* 103, 146-162.

Eglinton, T. I., Aluwihare, L. I., Bauer, J. E., Druffel, E. R. M., and McNichol, A. P., 1996. Gas chromatographic isolation of individual compounds from complex matrices for radiocarbon dating. *Analytical Chemistry* 68, 904-912.

France-Lanord, C. and Derry, L. A., 1997. Organic carbon burial forcing of the carbon cycle from Himalayan erosion. *Nature* 390, 65-67.

Furukawa, Y., 2000. Energy-filtering transmission electron microscopy (EFTEM) and electron energy-loss spectroscopy (EELS) investigation of clay-organic matter aggregates in aquatic sediments. *Organic Geochemistry* 31, 735-744.

Gaillardet, J., Dupré, B., Louvat, P., and Allègre, C. J., 1999. Global silicate weathering and CO_2 consumption rates deduced from the chemistry of large rivers. *Chemical Geology* 159, 3-30.

Gajurel, A. P., France-Lanord, C., Huyghe, P., Guilmette, C., and Gurung, D., 2006. C and O isotope compositions of modern fresh-water mollusc shells and river waters from the Himalaya and Ganga plain. *Chemical Geology* 233, 156-183.

Galy, A. and France-Lanord, C., 1999. Weathering processes in the Ganges-Brahmaputra basin and the riverine alkalinity budget. *Chemical Geology* 159, 31-60.

Galy, A. and France-Lanord, C., 2001. Higher Erosion rates in the Himalaya: geochemical constraints on riverine fluxes. *Geology* 29, 23-26.

Galy, V., Bouchez, J., and France-Lanord, C., 2007a. Determination of total organic carbon content and $\delta^{13}\text{C}$ in carbonate rich detrital sediments. *Geostandards and Geoanalytical research* 31, 199-207. 10.1111/j.1751-908X.2007.00864.x

Galy, V., France-Lanord, C., Beyssac, O., Faure, P., Kudrass, H., and Palhol, F., 2007b. Efficient organic carbon burial in the Bengal fan sustained by the Himalayan erosional system. *Nature* 450, 407-410.

Galy, V., François, L., France-Lanord, C., Faure, P., Kudrass, H., Palhol, F., and Singh, S. K., Submitted. C_4 plants decline in the Himalayan basin since the Last Glacial Maximum. *Quaternary Science Reviews*.

Goni, M. A., Monacci, N., Gisewhite, R., Ogston, A., Crockett, J., and Nittrouer, C., 2006. Distribution and sources of particulate organic matter in the water column and sediments of the Fly River Delta, Gulf of Papua (Papua New Guinea). *Estuarine, Coastal and Shelf Science* 69, 225-245.

Hedges, J. I. and Keil, R. G., 1995. Sedimentary organic matter preservation: an assessment and speculative synthesis. *Marine Chemistry* 49, 81-115.

Hedges, J. I., Keil, R. G., and Benner, R., 1997. What Happens to terrestrial organic matter in the ocean? *organic Geochemistry* 27, 195-212.

Hedges, J. I. and Oades, J. M., 1997. Comparative organic geochemistries of soils and marine sediments. *Organic Geochemistry* 27, 319-361.

800 Heroy, D. C., Kuehl, S. A., and Goodbred, J., Steven L., 2003. Mineralogy of the Ganges and Brahmaputra Rivers: implications for river switching and Late Quaternary climate change. *Sedimentary Geology* 155, 343-359.

Hilton, R. G., Galy, A., and Hovius, N., in press. Riverine particulate organic carbon from an active mountain belt: The importance of landslides. *Global Biogeochemical Cycles*.

Islam, G. M. T. and Jaman, S. T., 2006. Modeling sediment loads in the lower Ganges, Bangladesh. *Water Management* 159, 87-94.

810 Keil, R. G., Mayer, L. M., Quay, P. D., Richey, J. E., and Hedges, J. I., 1997. Loss of organic matter from riverine particulates in deltas. *Geochimica et Cosmochimica Acta* 61, 1507-1511.

Lasaga, A. C., Berner, R. A., and Garrels, R. M., 1985. An improved geochemical model of atmospheric CO₂ fluctuations over the past 100 million years. In: Sundquist, E. T. and Broecker, W. S. Eds.), *The Carbon Cycle and Atmospheric CO₂: Natural Variations Archean to Present*. AGU, Washington.

820 Le Fort, P., 1989. The Himalayan orogenic segment. In: Sengör, A. M. C. (Ed.), *Tectonic evolution of the Tethyan regions*. Proceedings of the NATO ASI meeting, Istanbul, October 1985., Reidel Publ. Co.

Ludwig, W., Probst, J.-L., and Kempe, S., 1996. Predicting the oceanic input of organic carbon by continental erosion. *Global Biogeochemical Cycles* 10, 23-41.

Mackenzie, F. T., 1981. Global carbon cycle: some minor sink for CO₂. In: Likens, G. E., Mackenzie, F. T., Richey, J. E., Sedell, J. R., and Turekian, K. K. Eds.), *Flux of organic carbon by rivers to the ocean*. U.S. Department of Energy, Washington, D.C.

830 Mayer, L. M., 1994. Surface area control of organic carbon accumulation in continental shelf sediments. *Geochimica et Cosmochimica Acta* 58, 1271-1284.

Mayer, L. M., 1999. Extent of coverage of mineral surfaces by organic matter in marine sediments. *Geochimica et Cosmochimica Acta* 63, 207-215.

Mayer, L. M., Schick, L. L., Hardy, K. R., Wagai, R., and McCarthy, J., 2004. Organic matter in small mesopores in sediments and soils. *Geochimica et Cosmochimica Acta* 68, 3863-3872.

840 Mook, W. G. and Tan, F. C., 1991. Stable carbon isotopes in rivers and estuaries. In: Degens, E. T., Kempe, S., and Richey, J. E. Eds.), *Biogeochemistry of Major World Rivers*.

Park, Y. A. and Khim, B. K., 1992. Origin and dispersal of recent clay minerals in the Yellow Sea. *Marine Geology* 104, 205-213.

Ruddiman, W. F., 1997. Tectonic uplift and climate change. Plenum, New York.

Sauer, P. E., Eglinton, T. I., Hayes, J. M., Schimmelmann, A., and Sessions, A. L., 2001. Compound-specific D/H ratios of lipid biomarkers from sediments as a proxy for environmental and climatic conditions. *Geochimica et Cosmochimica Acta* 65, 213-222.

Schlünz, B. and Schneider, R. R., 2000. Transport of terrestrial organic carbon to the oceans by rivers: re-estimating flux and burial rates. *International Journal of Earth Sciences* 88, 599-606.

Scott, D. T., Baisden, W. T., Davies-Colley, R., Gomez, B., Hicks, D. M., Page, M. J., Preston, N. J., Trustrum, N. A., Tate, K. R., and Woods, R. A., 2006. Localized erosion affects national carbon budget. *Geophysical Research Letters* 33, 1-4.

Singh, M., Sharma, M., and Tobschall, H. J., 2005a. Weathering of the Ganga alluvial plain, northern India: implications from fluvial geochemistry of the Gomati River. *Applied Geochemistry* 20, 1-21.

Singh, S. and France-Lanord, C., 2002. Tracing the distribution of erosion in the Brahmaputra watershed from isotopic compositions of stream sediments. *Earth and Planetary Science Letters* 252, 645-662.

Singh, S. K., Sarin, M. M., and France-Lanord, C., 2005b. Chemical erosion in the eastern Himalaya: Major ion composition of the Brahmaputra and $\delta^{13}\text{C}$ of dissolved inorganic carbon. *Geochimica et Cosmochimica Acta* 69, 3573-3588.

Sinha, R., Jain, V., Babu, G. P., and Ghosh, S., 2005. Geomorphic characterization and diversity of the fluvial systems of the Gangetic Plains. *Geomorphology* 70, 207-225.

Sollins, P., Homann, P., and Caldwell, B. A., 1996. Sabilization and destabilization of soil organic matter: mechanisms and controls. *Geoderma* 74, 65-105.

Subramanian, V. and Ittekkot, V., 1991. Carbon Transport by the Himalayan Rivers. In: Degens, E. T., Kempe, S., and Richey, J. E. Eds.), *Biogeochemistry of Major World Rivers*.

Sundquist, E. T., 1985. Geological perspectives on carbon dioxide. In: Sundquist, E. T. and Broecker, W. S. Eds.), *The Carbon Cycle and Atmospheric CO₂: Natural Variations Archean to Present*. AGU, Washington.

Wagai, R. and Mayer, L. M., 2007. Sorptive stabilization of organic matter in soils by hydrous iron oxides. *Geochimica et Cosmochimica Acta* 71, 25-35.

Table 1: Chemical composition, organic carbon composition, specific area and grain size of river sediments from the Ganga-Brahmaputra basin.

Sample #	River	Locality	Latitude		Longitude		Type	Date	TSS	Al/Si	TOC*	$\delta^{13}C_{org}$	SA	External SA	< 25 μm
			°N	min	°E	min	depth (m)		g/l	mol:mol	%	‰	m ² /g	m ² /g	% v
Ganga basin															
PB 76	Rapti	Bahlabang	27	50.2	82	32.4	SL surf	14/07/05	2.6	0.22	0.27	-24.4			
MO 315	Kali		27	54.2	83	89.2	SL surf	08/07/98		0.24	0.27	-25.0			
PB 61	Kali	confluence	27	44.5	84	25.3	SL surf	11/07/05	4.4	0.24	0.33	-24.9			
MO 305	Seti		28	3.0	84	4.5	SL surf			0.29	0.20	-22.4			
MO 301	Trisuli	Benighat	27	48.6	84	46.8	SL surf			0.30	0.31	-24.7			
PB 82	Trisuli		27	48.6	84	50.2	SL surf	14/07/05	0.5	0.36	0.52	-24.4			
PB 72	Karnala Nadi	Highway bg.	26	52.7	86	8.5	SL surf	13/07/05	1.1	0.34	0.83	-25.5			
PB 73	Karnala Nadi	Highway bg.	26	52.7	86	8.3	SL surf	13/07/05	5.3	0.10	0.20	-25.6			
BR 133	Gomati		25	34.6	82	59.8	Bank	09/08/01		0.28	0.63	-21.9			
Trans-Himalayan rivers															
PB 79	Karnali	Chisapani	28	38.5	81	17.0	SL surf	15/07/05	1.3	0.21	0.41	-25.6			45.1
PB 80	Karnali	Chisapani	28	40.7	81	17.1	Bank	15/07/05		0.10	0.02	-23.6			
BR 356	Ghaghara	Ayodia	26	48.8	82	12.2	Bank	15/05/04		0.30	0.29	-23.0			
BR 372	Ghaghara	Dohrighat	26	16.5	83	30.8	Bank	16/05/04		0.24	0.24	-23.2			
BR 344	Ghaghara	Revelganj	25	49.2	84	35.1	Bank	12/05/04		0.27	0.26	-23.0			
MO 331	Narayani	Narayanghat	27	41.4	84	23.7	SL surf			0.24	0.22	-24.4			
MO 217	Narayani	Narayanghat	27	41.4	84	23.7	BL	20/05/97		0.15	0.08	-23.8			
NAG 48 †	Narayani	Narayanghat	27	41.4	84	23.7	Bank			0.15	0.11	-24.0			
PB 60	Narayani	Narayanghat	27	42.2	84	25.6	SL surf*	11/07/05		0.27	0.34	-24.5			
PB 58	Narayani	Narayanghat	27	42.2	84	25.6	SL surf	11/07/05	2.9	0.27	0.33	-24.7			53.9
PB 57	Narayani	Narayanghat	27	42.2	84	25.6	SL 2 m	11/07/05	4.8	0.23	0.24	-24.3			37.2
PB 56	Narayani	Narayanghat	27	42.2	84	25.6	SL 4 m	11/07/05	5.6	0.22	0.21	-24.3			25.1
PB 55	Narayani	Narayanghat	27	42.2	84	25.6	SL 6 m	11/07/05	9.1	0.21	0.20	-24.3			26.1
PB 54	Narayani	Narayanghat	27	42.2	84	25.6	SL 8 m	11/07/05	10.2	0.19	0.18	-24.2			19.4
BR 335	Gandak	Barauli	26	21.6	84	44.7	Bank	11/05/04		0.22	0.26	-23.3			
BR 113	Gandak	Hajipur	25	41.3	85	11.3	SL surf	05/08/01	1.2	0.31	0.59	-23.9			
BR 114	Gandak	Hajipur	25	41.3	85	11.3	SL 1.5 m	05/08/01		0.27	0.32	-23.8			
BR 117	Gandak	Hajipur	25	41.3	85	11.3	Bank	05/08/01		0.16	0.11	-22.6			
PB 65	Kosi	Chatra	26	50.8	87	9.1	SL 3.8 m	13/07/05	5.7	0.30	0.32	-25.2			36.3
PB 66	Kosi	Chatra	26	50.8	87	9.1	SL 2.8 m	13/07/05	3.4	0.30	0.35	-25.4			44.3
PB 67	Kosi	Chatra	26	50.8	87	9.1	SL 1 m	13/07/05	2.8	0.33	0.40	-25.4			48.2
PB 68	Kosi	Chatra	26	50.8	87	9.1	SL surf	13/07/05	2.6	0.32	0.42	-25.5			48.7
PB 70	Kosi	Chatra	26	50.8	87	9.1	Bank	13/07/05		0.14	0.05	-23.6			
BR 331	Kosi	Dumarighat	25	32.4	86	43.3	Bank	10/05/04		0.31	0.33	-21.8			
BR 102	Kosi	confluence	25	25.1	87	13.7	SL 6.5 m	05/08/01		0.22	0.14	-23.5			
BR 103	Kosi	confluence	25	25.1	87	13.7	BL	05/08/01		0.16	0.04	-23.3			
Mainstream															
BR 351	Ganga	Allahabad	25	26.0	81	53.0	Bank	14/05/04		0.29	0.32	-21.6			
BR 140	Ganga	Varanasi	25	18.4	83	0.6	SL 1.5 m	10/08/01	0.4	0.32	0.73	-21.2			
BR 139	Ganga	Varanasi	25	18.1	83	0.5	SL 3 m	10/08/01	0.7	0.31	0.72	-21.2			
BR 138	Ganga	Varanasi	25	18.3	83	0.6	SL 6 m	10/08/01	1.1	0.25	0.54	-21.3			
BR 137	Ganga	Varanasi	25	18.1	83	0.5	SL 8 m	10/08/01	1.5	0.19	0.36	-21.3			
BR 136	Ganga	Varanasi	25	17.9	83	0.6	BL 4.5 m	10/08/01		0.09	0.02	-25.0			
BR 144	Ganga	Varanasi	25	19.1	83	1.5	BL 15 m	10/08/01		0.15	0.05	-23.9			
BR 122	Ganga	Patna	25	37.4	85	9.2	SL 1.5 m	08/08/01	1.0	0.28	0.56	-22.1			64.9
BR 120	Ganga	Patna	25	37.5	85	9.1	SL 3.5 m	08/08/01	1.2	0.25	0.56	-22.2			55.9
BR 119	Ganga	Patna	25	37.5	85	9.0	SL 5.2 m	08/08/01	1.1	0.27	0.53	-21.9			59.1
BR 121	Ganga	Patna	25	37.4	85	9.1	SL 6.1 m	08/08/01	1.1	0.27	0.54	-22.0			62.5
BR 125	Ganga	Patna	25	37.4	85	8.8	SL 6.2 m	08/08/01	0.5	0.40	0.96	-22.0			80.9
BR 118	Ganga	Patna	25	37.5	85	9.1	SL 7.8 m	08/08/01	3.1	0.15	0.21	-22.6			14.6
BR 124	Ganga	Patna	25	37.4	85	8.8	BL 7 m	08/08/01		0.11	0.03	-24.3			1.4
BR 303	Ganga	Patna	25	37.4	85	9.1	SL 6.7 m	07/05/04	0.2	0.12	0.20	-26.4			
BR 304	Ganga	Patna	25	37.4	85	9.1	SL 3.4 m	07/05/04	0.2	0.12	0.21	-26.2			
BR 306	Ganga	Patna	25	37.4	85	9.1	Bank	07/05/04		0.10	0.03	-24.3			
BR 314	Ganga	Barauni	25	22.8	85	59.9	Bank	08/05/04		0.29	0.42	-22.5			
BR 109	Ganga	Manihari	25	18.5	87	36.0	SL 1.5 m	06/08/01	1.1	0.30	0.57	-21.8			
BR 108	Ganga	Manihari	25	18.5	87	36.0	SL 5.2 m	06/08/01	1.2	0.29	0.61	-22.4			
BR 107	Ganga	Manihari	25	18.2	87	36.2	SL 10.8 m	06/08/01	2.3	0.25	0.53	-22.7			
BR 106	Ganga	Manihari	25	18.1	87	36.3	Bank	06/08/01		0.13	0.07	-23.3			
BR 104	Ganga	Manihari	25	19.0	87	36.2	SL 4.3 m	06/08/01	3.1	0.22	0.42	-22.3			
BR 105	Ganga	Manihari					SL 5.6 m	06/08/01		0.17	0.26	-22.7			
BGP 7 †	Ganga	Rajshahi	24	21.5	88	36.5	SL surf	02/08/93	1.1	0.37	0.71	-21.7			
BGP 5 †	Ganga	Rajshahi	24	21.5	88	36.5	BL	02/08/93		0.21	0.19	-22.3			
BGP 6 †	Ganga	Rajshahi	24	21.5	88	36.5	BL	02/08/93		0.12	0.05	-24.5			
BGP 68	Ganga	Rajshahi	24	21.5	88	36.5	BL	02/08/93		0.11	0.05	-23.5			
BR 212	Ganga	Harding bridge	24	3.7	89	1.6	SL 1 m	16/07/02	0.6	0.38	0.66	-22.0			81.9
BR 211	Ganga	Harding bridge	24	3.6	89	1.7	SL 3.5 m	16/07/02	0.8	0.34	0.62	-22.4			74.9
BR 209	Ganga	Harding bridge	24	3.8	89	1.6	SL 5 m	16/07/02	0.7	0.35	0.67	-22.3			75.5
BR 208	Ganga	Harding bridge	24	3.8	89	1.6	SL 10 m	16/07/02	0.7	0.34	0.62	-22.1			71.9
BR 210	Ganga	Harding bridge	24	3.8	89	1.6	SL 17 m	16/07/02	1.2	0.28	0.47	-22.4			52.8
BR 214	Ganga	Harding bridge	24	3.6	89	1.7	BL 22 m	16/07/02		0.14	0.10	-22.8			12.4
BR 417	Ganga	Harding bridge	24	1.4	89	2.0	SL surf*	13/07/04		0.38	0.53	-21.0			80.5
BR 415	Ganga	Harding bridge	24	1.4	89	2.0	SL surf	13/07/04	0.8	0.38	0.53	-21.1			77.8
BR 414	Ganga	Harding bridge	24	1.3	89	2.1	SL 2 m	13/07/04	1.0	0.33	0.46	-20.9			69.4
BR 413	Ganga	Harding bridge	24	1.3	89	2.3	SL 4 m	13/07/04	1.3	0.29	0.42	-20.6			62.0
BR 412	Ganga	Harding bridge	24	1.4	89	2.4	SL 6.5 m	13/07/04	1.5	0.28	0.38	-21.2			55.1
BR 411	Ganga	Harding bridge	24	1.5	89	2.3	SL 9 m	13/07/04	2.9	0.21	0.22	-21.4			31.8
BR 418	Ganga	Harding bridge	24	1.4	89	2.0	BL 10 m	13/07/04		0.13	0.03	-22.7			1.2
BR 515	Ganga	Harding bridge	24	2.3	89	2.0	SL surf	23/07/05	0.9	0.37	0.71	-20.7	34.8	26.0	86.5
BR 514	Ganga	Harding bridge	24	2.3	89	2.0	SL 2.5 m	23/07/05	1.4	0.32	0.57	-20.6			
BR 513	Ganga	Harding bridge	24	2.3	89	2.0	SL 5 m	23/07/05	1.7	0.28	0.45	-21.0	21.3	16.7	65.8
BR 512	Ganga	Harding bridge	24	2.3	89	2.0	SL 7 m	23/07/05	1.8	0.27	0.42	-21.0			
BR 511	Ganga	Harding bridge	24	2.3	89	2.0	SL 10 m	23/07/05	2.4	0.24	0.32	-21.4	17.4	13.7	46.3
BR 516	Ganga	Harding bridge	24	2.3	89	2.0	BL 11 m	23/07/05		0.13	0.05	-22.4	1.3	1.0	3.7
BR 519	Ganga	Harding bridge	24	2.5	89	2.2	SL surf	23/07/05	0.7	0.41	0.82	-20.8			
BR 518	Ganga	Harding bridge	24	2.5	89	2.2	SL 5 m	23/07/05	1.5	0.31	0.53	-20.9			69.6
BR 517	Ganga	Harding bridge	24	2.5	89	2.2	SL 9.8 m	23/07/05	1.8	0.28	0.47	-20.8			
BR 520	Ganga	Harding bridge	24	2.5	89	2.2	BL 10 m	23/07/05		0.17	0.14	-22.3			
BR 522	Ganga	Harding bridge	24	2.5	89	2.2	SL surf*	23/07/05		0.40	0.70	-20.0			

Table 1 (continued)

Sample #	River	Locality	Latitude		Longitude		Type	Date	TSS	Al/Si	TOC*	$\delta^{13}\text{C}_{\text{org}}$	SA	External SA	< 25 μm
			°N	min	°E	min	depth (m)		g/l	mol:mol	%	‰	m ² /g	m ² /g	% v
Brahmaputra basin															
Secondary tributaries															
BR 25	Ranga Nadi		27	12.2	94	3.5	Bank	29/10/99		0.12	0.31	-24.1			
BR 58	Ranga Nadi		27	12.3	94	3.6	Bank	27/07/01		0.10	0.15	-23.6			
BR 35	Puthimari		26	22.0	91	39.2	Bank	30/10/99		0.15	1.26	-22.8			
BR 69	Puthimari		26	22.0	91	39.2	SL surf	30/07/01		0.28	1.50	-23.6			
BR 70	Puthimari		26	22.0	91	39.2	Bank	30/07/01		0.15	0.88	-23.3			
BR 76	Tipkai		26	13.1	90	8.3	Bank	30/07/01		0.09	0.02	-21.1			
BR 27	Jia Bhareli		26	48.6	92	52.6	Bank	29/10/99		0.15	0.34	-22.5			
BR 63	Jia Bhareli		26	48.6	92	52.8	SL surf	29/07/01		0.22	1.16	-24.5			
BR 64	Jia Bhareli		26	48.6	92	52.8	Bank	29/07/01		0.12	0.60	-23.2			
Trans-Himalayan rivers															
BR 59	Siang		28	4.7	95	20.2	SL surf	28/07/01		0.26	0.33	-23.7			
BR 60	Siang		28	4.7	95	20.2	Bank	28/07/02		0.18	0.05	-19.9			
BR 21	Subansiri		27	26.9	94	15.1	Bank	28/10/99		0.12	0.15	-22.5			
BR 61	Subansiri		27	26.7	94	15.4	SL surf	28/07/01		0.28	0.77	-26.3			
BR 62	Subansiri		27	26.7	94	15.4	Bank	28/07/01		0.14	0.17	-22.6			
BR 33	Manas		26	29.7	90	55.0	Bank	30/10/99		0.14	0.15	-23.8			
BR 71	Manas		26	29.7	90	55.2	SL surf	30/07/01		0.25	0.45	-24.5			
BR 72	Manas		26	29.7	90	55.2	Bank	30/07/01		0.13	0.09	-22.6			
BGP 11 †	Tista	Kaunia	25	47.5	89	26.2	Bank	04/08/93		0.20	0.10	-23.7			
BGP 76	Tista	Kaunia	25	47.5	89	26.2	Bank	07/03/94		0.24	0.15	-23.7			
Mainstream															
BR 29	Brahmaputra	Tezpur bg.	26	36.7	92	51.2	Bank	29/10/03		0.16	0.13	-22.9			
BR 65	Brahmaputra	Tezpur bg.	26	36.7	92	51.2	SL surf	29/07/01		0.30	0.82	-24.3			
BR 66	Brahmaputra	Tezpur bg.	26	36.7	92	51.2	BL	29/07/01		0.18	0.13	-22.4			
BR 8	Brahmaputra	Guwahati	26	11.2	91	44.3	SL 5 m	25/10/99	1.2	0.26	0.46	-25.5			
BR 7	Brahmaputra	Guwahati	26	11.2	91	44.3	SL 5 m	25/10/99	2.5	0.22	0.21	-25.3			
BR 6	Brahmaputra	Guwahati	26	11.6	91	44.2	SL surf	25/10/99	0.8	0.32	0.74	-24.7			
BR 2	Brahmaputra	Guwahati	26	11.5	91	44.4	SL 5 m	25/10/99		0.25	0.46	-24.9			
BR 4	Brahmaputra	Guwahati	26	11.6	91	44.2	SL 10.5 m	25/10/99	1.8	0.24	0.30	-24.7			
BR 3	Brahmaputra	Guwahati	26	11.5	91	44.4	SL 11 m	25/10/99	0.8	0.28	0.49	-24.5			
BR 9	Brahmaputra	Guwahati	26	11.6	91	45.0	Bank	25/10/99		0.18	0.08	-23.1			
BR 55	Brahmaputra	Guwahati	26	11.6	91	44.2	SL surf	26/07/01		0.32	0.62	-23.9			
BR 54	Brahmaputra	Guwahati	26	11.6	91	44.2	SL 5 m	26/07/01		0.32	0.67	-23.9			
BR 53	Brahmaputra	Guwahati	26	11.6	91	44.2	SL 10 m	26/07/01		0.22	0.37	-23.8			
BR 52	Brahmaputra	Guwahati	26	11.6	91	44.2	SL 15 m	26/07/01		0.22	0.29	-23.7			
BR 56	Brahmaputra	Guwahati	26	11.6	91	44.2	BL	26/07/01		0.19	0.09	-23.4			
BR 73	Brahmaputra	Dhubri	26	1.1	89	59.8	SL surf	30/07/01		0.33	0.68	-23.5			
BR 74	Brahmaputra	Dhubri	26	1.1	89	59.8	BL	30/07/01		0.16	0.05	-22.3			
BGP 18 †	Brahmaputra	Chilmari	25	33.0	89	43.2	SL surf	05/08/96	0.4	0.33	0.59	-23.0			
BGP 82 †	Brahmaputra	Chilmari	25	33.0	89	43.2	BL	07/03/94		0.16	0.05	-22.2			
BGP 14 †	Brahmaputra	Chilmari	25	33.0	89	43.2	BL	05/08/93		0.19	0.22	-22.9			
BR 401	Brahmaputra	Sirajganj	24	28.4	89	43.6	SL 6.5 m	11/07/04	4.3	0.23	0.26	-23.3			25.2
BR 405	Brahmaputra	Sirajganj	24	27.5	89	43.7	SL 5 m	12/07/04	6.0	0.22	0.22	-23.2			17.8
BR 406	Brahmaputra	Sirajganj	24	27.6	89	43.7	SL 3 m	12/07/04	3.1	0.24	0.32	-22.0			36.1
BR 407	Brahmaputra	Sirajganj	24	28.0	89	43.5	11 m	12/07/04	6.4	0.22	0.26	-23.0	3.6	3.6	19.0
BR 408	Brahmaputra	Sirajganj	24	28.1	89	43.5	SL 1.5 m	12/07/04	1.8	0.29	0.44	-23.0			51.8
BR 409	Brahmaputra	Sirajganj	24	28.1	89	43.5	SL surf	12/07/04	1.3	0.32	0.54	-23.1	7.6	7.6	65.8
BR 402	Brahmaputra	Sirajganj	24	28.4	89	43.6	SL surf*	11/07/04		0.32	0.50	-22.5			65.4
BR 459	Brahmaputra	Sirajganj	24	28.2	89	43.9	SL surf*	23/07/04		0.37	0.64	-23.9			87.2
BR 457	Brahmaputra	Sirajganj	24	28.5	89	43.7	SL surf	23/07/04	1.3	0.36	0.69	-23.9			81.4
BR 456	Brahmaputra	Sirajganj	24	28.4	89	43.6	SL 3 m	23/07/04	2.9	0.28	0.45	-23.5			50.6
BR 455	Brahmaputra	Sirajganj	24	28.0	89	43.8	SL 6 m	23/07/04	2.4	0.29	0.50	-23.9			54.7
BR 454	Brahmaputra	Sirajganj	24	28.3	89	43.5	SL 9 m	23/07/04	6.2	0.22	0.29	-23.6			23.6
BR 460	Brahmaputra	Sirajganj	24	28.4	89	43.7	BL 10 m	23/07/04		0.17	0.04	-22.1			1.7
BR 450	Brahmaputra	Sirajganj	24	30.9	89	44.1	BL	23/07/04		0.31	0.68	-24.1			66.2
BR 453	Brahmaputra	Sirajganj	24	27.4	89	43.7	BL	23/07/04		0.22	0.19	-23.1			
BR 500	Brahmaputra	Sirajganj	89	44.6	24	28.6	SL surf*	21/07/05		0.31	0.58	-23.5			
BR 501	Brahmaputra	Sirajganj	89	44.6	24	28.6	SL 6.5 m	22/07/05	2.0	0.29	0.51	-23.7			44.2
BR 502	Brahmaputra	Sirajganj	89	44.6	24	28.6	SL 2.5 m	22/07/05	0.8	0.33	0.59	-23.9			
BR 503	Brahmaputra	Sirajganj	89	44.6	24	28.7	BL 7.5 m	22/07/05		0.18	0.11	-23.2	1.8	1.3	
BR 504	Brahmaputra	Sirajganj	89	43.9	24	28.4	SL 9.8 m	22/07/05	2.3	0.25	0.37	-24.3	5.2	5.2	39.8
BR 505	Brahmaputra	Sirajganj	89	43.7	24	28.4	SL 7 m	22/07/05	2.1	0.27	0.40	-23.9			55.4
BR 506	Brahmaputra	Sirajganj	89	43.8	24	28.4	SL 5 m	22/07/05	1.6	0.29	0.49	-23.4	6.5	6.5	
BR 507	Brahmaputra	Sirajganj	89	43.8	24	28.4	SL 2.8 m	22/07/05	1.4	0.32	0.53	-23.6			
BR 508	Brahmaputra	Sirajganj	89	43.8	24	28.4	SL surf	22/07/05	0.8	0.36	0.64	-24.1	8.9	8.9	78.1
BR 509	Brahmaputra	Sirajganj	89	43.8	24	28.4	BL 10 m	22/07/05		0.15	0.05	-21.8			1.4
BR 205	Brahmaputra	Sirajganj	24	23.9	89	47.8	SL surf	15/07/02	1.2	0.31	0.57	-23.0			64.3
BR 204	Brahmaputra	Sirajganj	24	24.2	89	47.8	SL 2 m	15/07/02		0.27	0.53	-23.4			50.0
BR 201	Brahmaputra	Sirajganj	24	23.4	89	47.8	SL 6 m	15/07/02		0.26	0.52	-23.6			44.3
BR 202	Brahmaputra	Sirajganj	24	23.1	89	47.9	SL 9.5 m	15/07/02	1.4	0.21	0.29	-23.0			16.4
BR 203	Brahmaputra	Sirajganj	24	23.0	89	47.9	SL 11.5 m	15/07/02	5.9	0.19	0.14	-23.3			
BR 206	Brahmaputra	Sirajganj	24	23.1	89	47.8	BL 12 m	15/07/02		0.20	0.06	-22.7			2.5
BR 207	Brahmaputra	Sirajganj					SL 1 m	15/07/02		0.23	0.25	-23.6			
BGP 3 †	Brahmaputra	Aricha Ghat	23	50.0	89	46.1	SL surf	01/08/96	0.3	0.37	0.72	-22.9			

SL = suspended sediment with depth of sampling, surf = surface sediment, * = sediment obtained by settling + filtration, BL = bed sediment.

SA = specific area, External SA = specific area corrected for the microporosity (see text)

TOC* and Al/Si of Bangladesh river sediments presented in this study are from Galy et al. (2007). Samples marked with a † are from Aucour et al (2006).

Table 2: Organic carbon content and stable isotopic composition of gravel samples from Himalayan rivers.

Sample #	River	Locality	Latitude		Longitude		Type	Lithology (a)	Al/Si at:at	TOC ⁺ %	$\delta^{13}\text{C}_{\text{org}}$ ‰
			°N	min	°E	min					
PB 5	Kali Gandaki	Jomsom	28	47.8	83	45.6		TSS	0.13	0.20	-22.0
PB 19	Lete Kola	confluence	28	37.6	83	37.2		HHC	0.24	0.01	-20.4
PB 22	Rukse Kola	confluence	28	33.3	83	38.3		HHC	0.21	0.08	-28.0
PB 28	Miristi Kola	confluence	28	30.9	83	39.8		HHC	0.23	0.02	-14.6
AR 67	Manas tributary		27	34.8	91	47.5		HHC	0.20	0.05	-22.5
MO 94	Jarang	Muchchok	28	3.5	84	39.5	gravel 2-4mm	LH	0.09	0.02	-24.8
MO 102	Marsel Kola	confluence	28	2.5	84	40.2		LH	0.16	0.02	-24.9
MO 112	Isul Kola	confluence	28	2.8	84	48.9		LH	0.09	0.07	-23.9
MAR 3	Marsyandi	Krishnebhir						LH	0.35	0.10	-17.0
AR 25	Tenga tributary		27	6.5	92	31.3		LH	0.18	0.02	-23.2
AR 32	Tenga tributary		27	9.8	92	33.6		LH	0.18	0.04	-27.0
Average (b)									0.19	0.04	-22.6

(a) Lithology refers to the main lithological unit drained upstream of each sampling site. TSS = Tibetan Sedimentary Series, HHC = High Himalaya Crystalline, LH = Lesser Himalaya.

(b) Average value was calculated as the arithmetic mean of the 11 samples.

FIGURE CAPTIONS

Figure 1: Map of the Himalayan basin showing the main rivers of the Ganga-Brahmaputra fluvial system and the location of sampling sites described in this study, identified either by sample number or locality name. Complete sample list and precise location are reported in Table 1. The Himalayan range, Tibetan plateau, Indian shield and Indo-Gangetic floodplain (white) are also shown.

Figure 2: Typical Transmitted Electron Microscope (a,b), binocular (c) and natural (d,e) photographs illustrating different forms and size of organic matter found in G-B river sediments. a: organo-mineral aggregate composed of granular organic matter (1) and phyllosilicate sheets (2) observed in surface suspended sediment of the Ganga. b: Micrometric polyphenol (brown pigment, 3) present as an independent particle of organic matter in surface suspended sediment of the Ganga. c: Plant macro-debris (4) observed in coarse suspended sediment sampled near the bottom of the Brahmaputra. d: Photograph of filtered suspended sediment sampled near the bottom of the Lower Meghna showing plant macro-debris (5). e: Large plant rafts floating at the surface of the Brahmaputra (Sirajganj, Bangladesh) during the 2005 monsoon.

Figure 3: Total C_{org} content of river sediments from the Ganga basin as a function of their Al/Si ratio. Different samplings define comparable positive linear relation between TOC^+ and Al/Si indicating similar control of the C_{org} loading in the basin. The slope of these trends characterises the C_{org} loading which is defined as $TOC^+/(Al/Si)$ (see Electronic Annex Table 1). The Ganga in the Western floodplain (Varanasi and Patna), the Karnali river as well as secondary tributaries have the highest C_{org} loading.

Figure 4: Total C_{org} content of river sediments from the Brahmaputra basin as a function of their Al/Si ratio. Different samplings define positive linear relation between TOC^+ and Al/Si ratio, the slope of these trends represents the C_{org} loading (see Electronic Annex Table 1). Brahmaputra and Trans-Himalayan rivers have comparable C_{org} loading while secondary tributaries clearly have higher C_{org} loading.

Figure 5: Evolution of grain size distribution with sampling depth for suspended (SL) and bed (BL) sediments of the Brahmaputra at Sirajganj (Bangladesh). Surface and bed sediments have unimodal distributions. Suspended sediments from intermediate depth have bimodal distributions forming a continuum between surface and bed sediment distributions.

Figure 6: Total C_{org} content of river sediments from the G-B system as a function of the proportion of fine ($< 25 \mu m$) particles. Different samplings define positive relation between TOC^+ and the proportion of fine particles. Best fit defined by sediments of Ganga (black line) and Brahmaputra (dashed line) in Bangladesh indicate comparable grain size control of the C_{org} content.

Figure 7: N_2 adsorption-desorption isotherms for surface suspended sediment of the Ganga and Brahmaputra in Bangladesh having similar Al/Si ratio. The shape of the isotherms for very low P/P_0 indicate different pore size distribution. Brahmaputra sediments have negligible proportion of micropores ($< 2 \text{ nm}$) while they account for ca. 20 % of the total specific area in Ganga sediments.

Figure 8: Total C_{org} content of Ganga and Brahmaputra bed (open symbol) and suspended (filled symbols) sediments in Bangladesh as a function of their total specific area. Suspended sediments of the Ganga (black line) and Brahmaputra (dashed line) define distinct trends corresponding to respective TOC^+/SA ratio of 0.73 ± 0.02 and $0.20 \pm 0.01 \text{ mgC g}^{-1}$.

Figure 9: Organic carbon stable isotopic composition ($\delta^{13}C_{org}$) of river sediments from the Ganga basin as a function of their TOC^+ . Trans-Himalayan rivers at the outflow of the Himalayan range and Ganga in the floodplain define distinct trends. C_{org} depleted bed sediments have quite similar $\delta^{13}C_{org}$ values while suspended sediments of the Ganga are 3 to 4 ‰ enriched in ^{13}C compared to that of Trans-Himalayan rivers.

Figure 10: Organic carbon stable isotopic composition ($\delta^{13}C_{org}$) of river sediments from the Brahmaputra basin as a function of their TOC^+ . Trans-Himalayan rivers at the outflow of the Himalayan range and Brahmaputra in the floodplain define comparable trends. C_{org} enriched suspended sediments have $\delta^{13}C_{org}$ values 1 to 2 ‰ lower than C_{org} depleted bed sediments.

Figure 11: Simplified map of the G-B fluvial system showing the evolution of $\delta^{13}C_{org}$ values from the Himalayan range to the delta. Bold numbers represent $\delta^{13}C_{org}$ values of surface suspended sediments; italic numbers represent $\delta^{13}C_{org}$ values of fine-grained bank sediments used as analogous of suspended sediments.

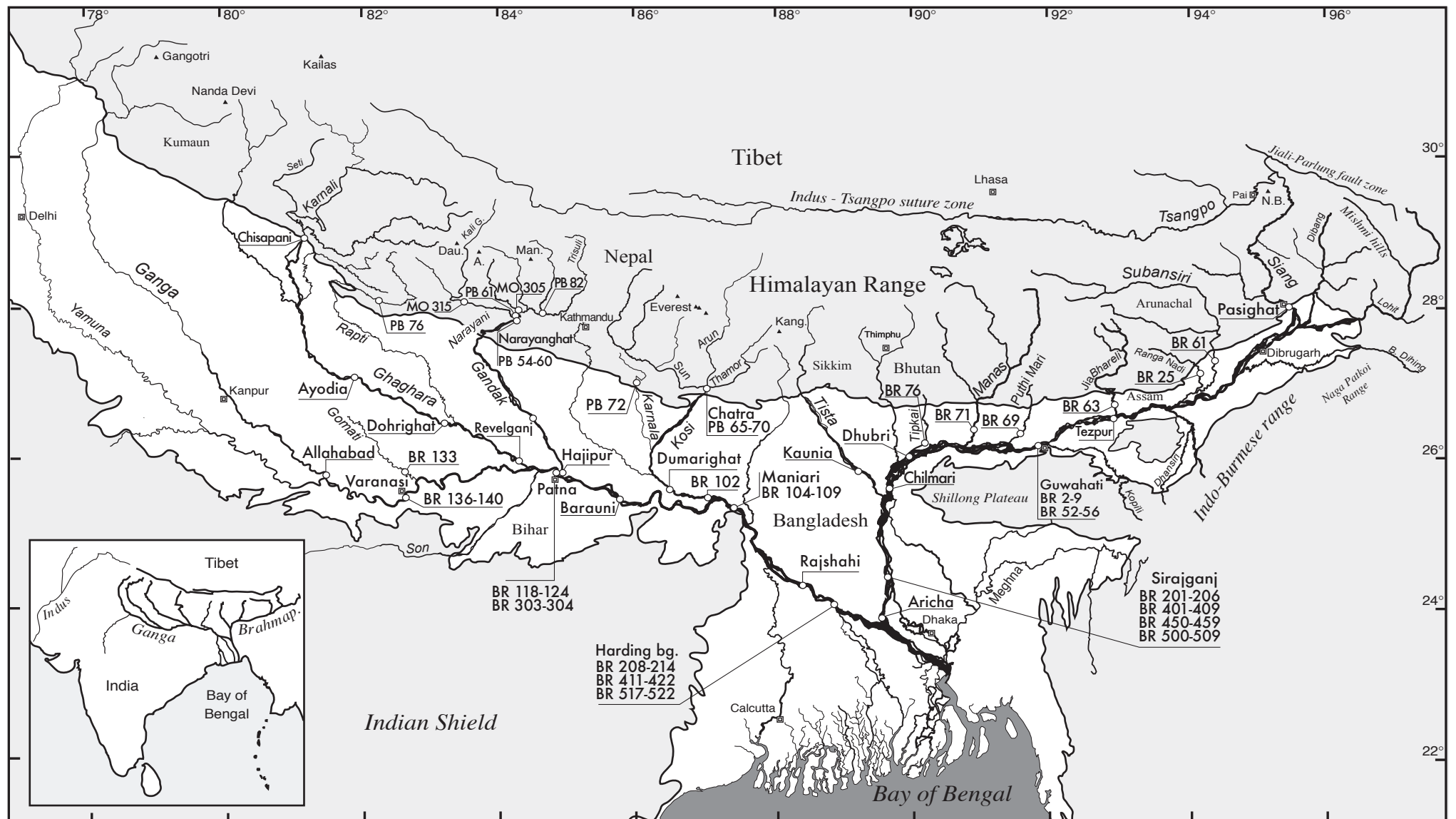


Figure 1

Figure 2

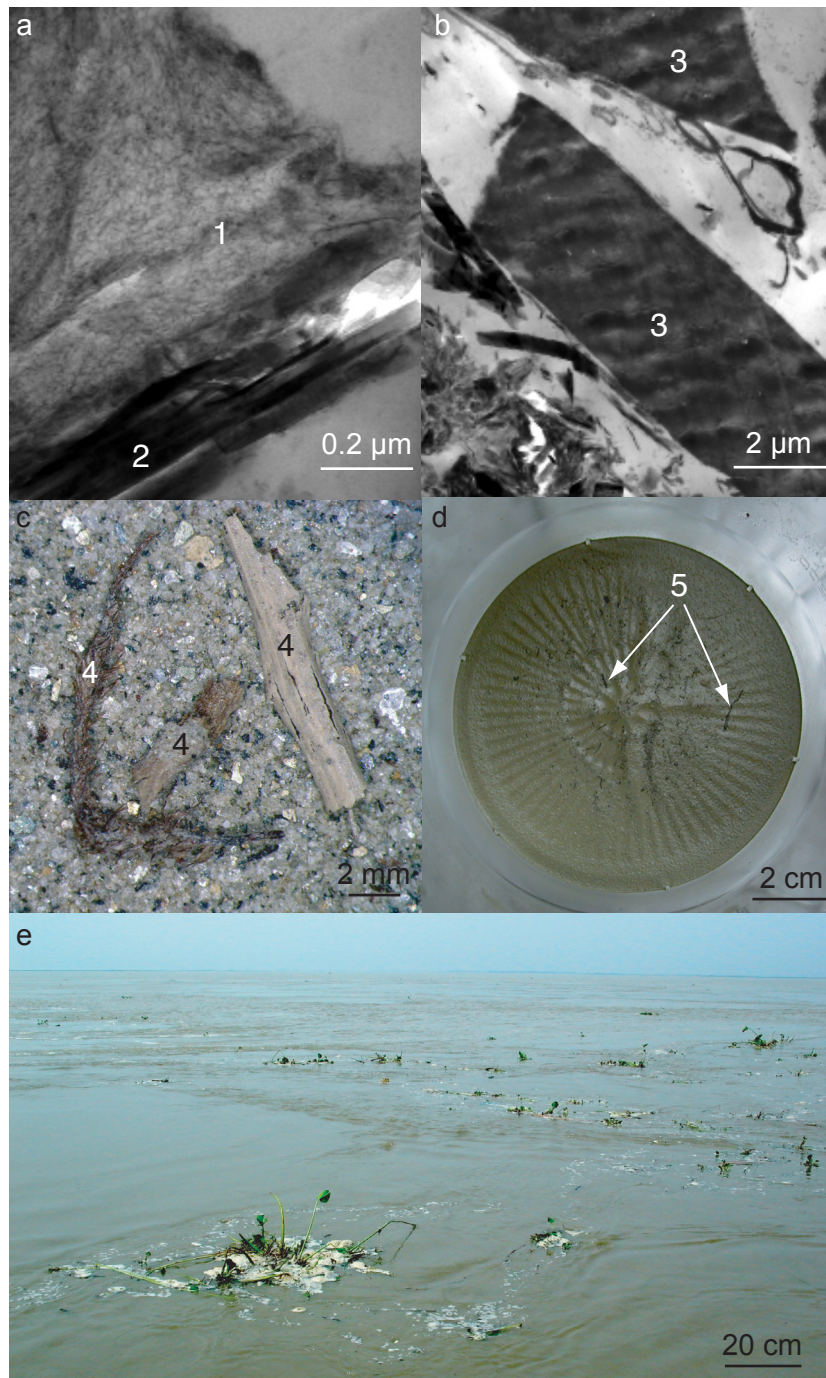


Figure 3

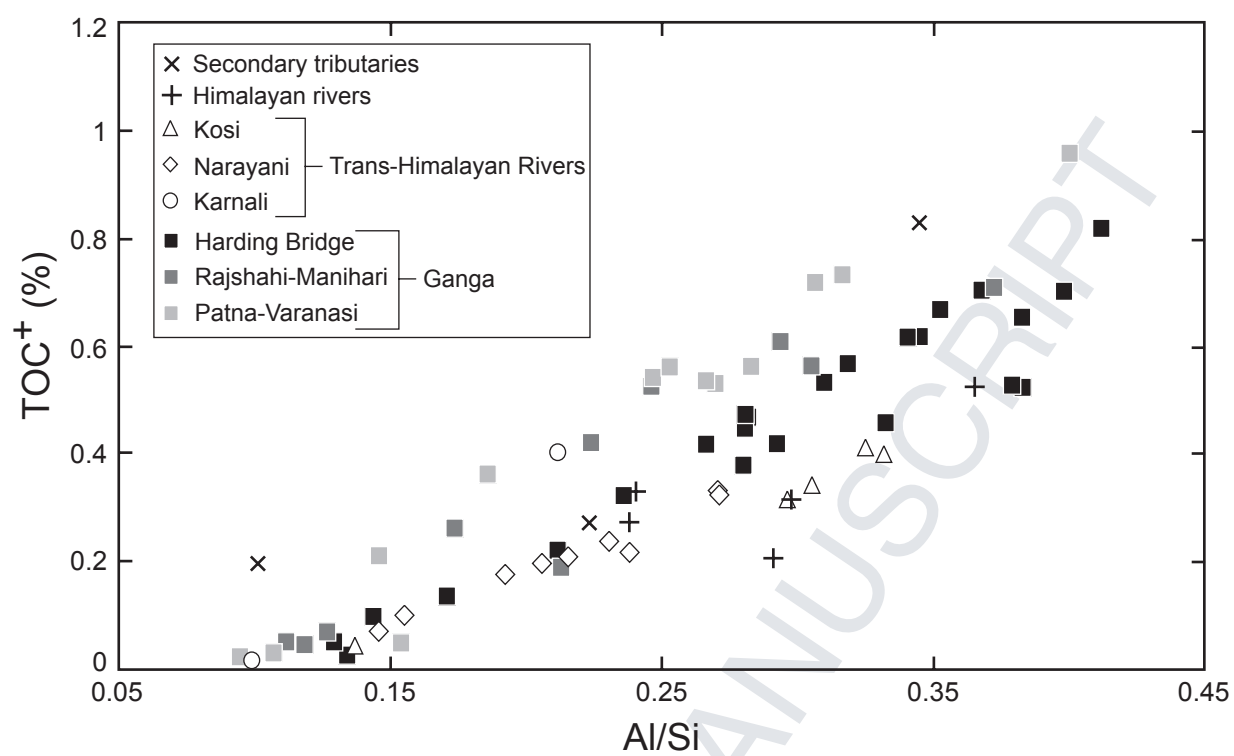


Figure 4

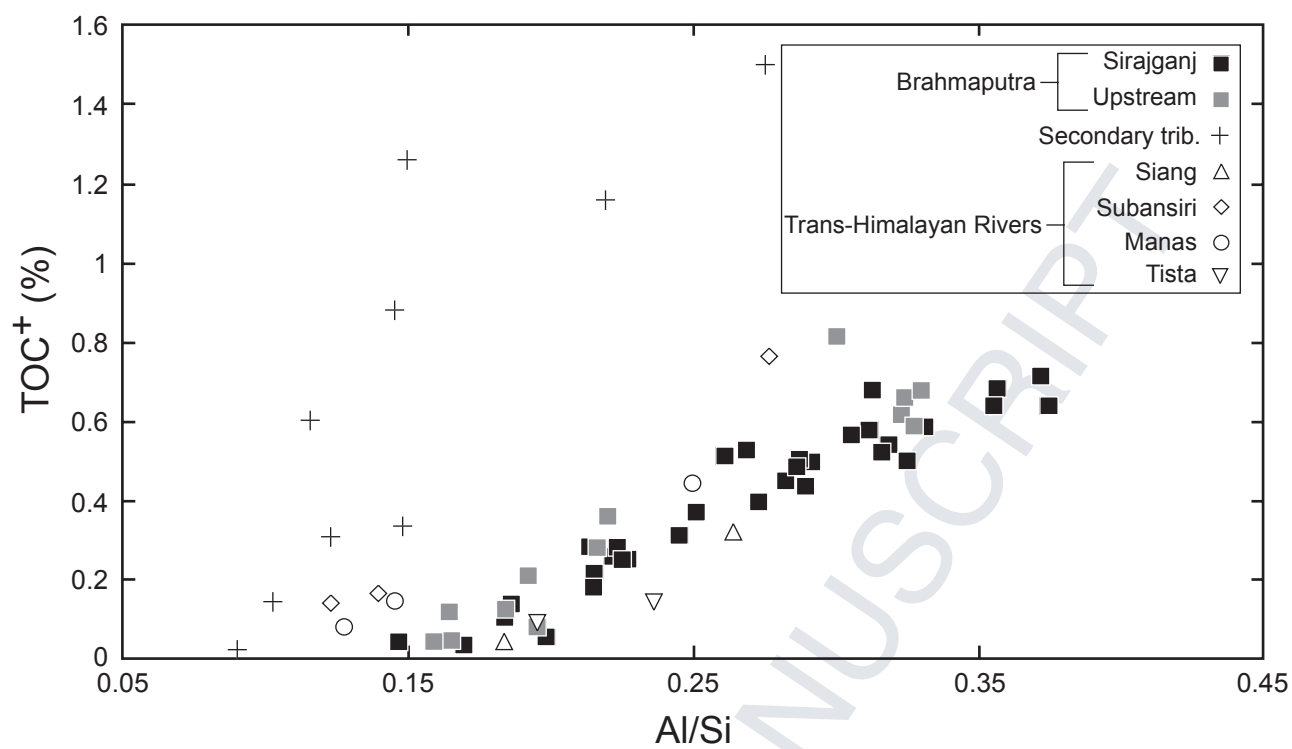


Figure 5

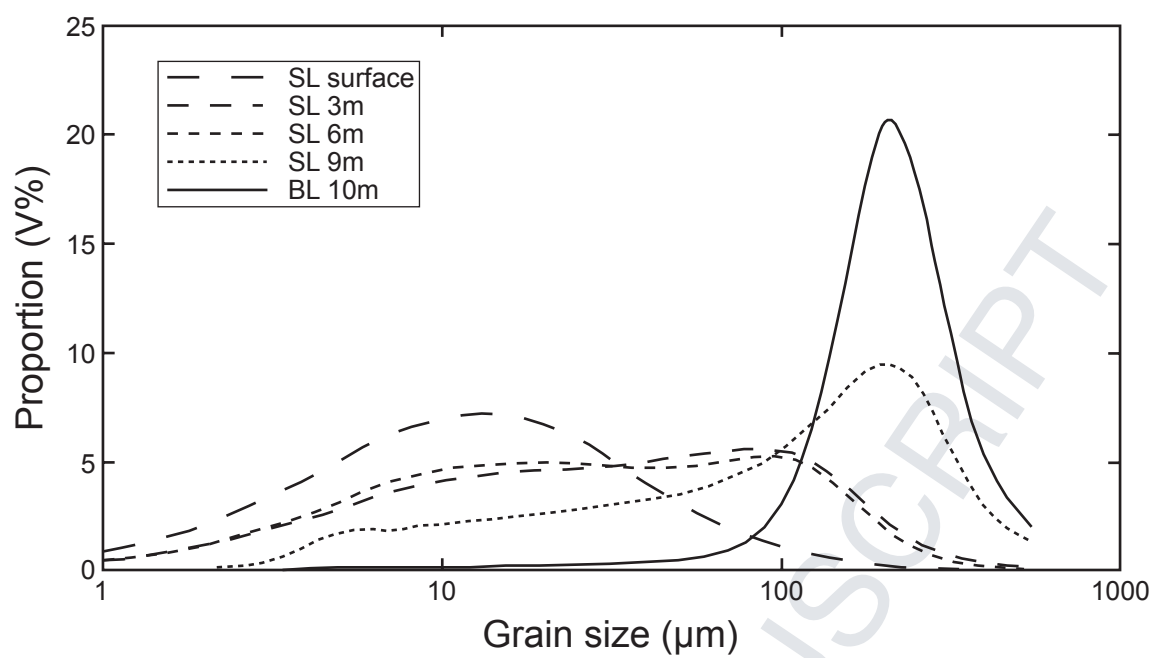


Figure 6

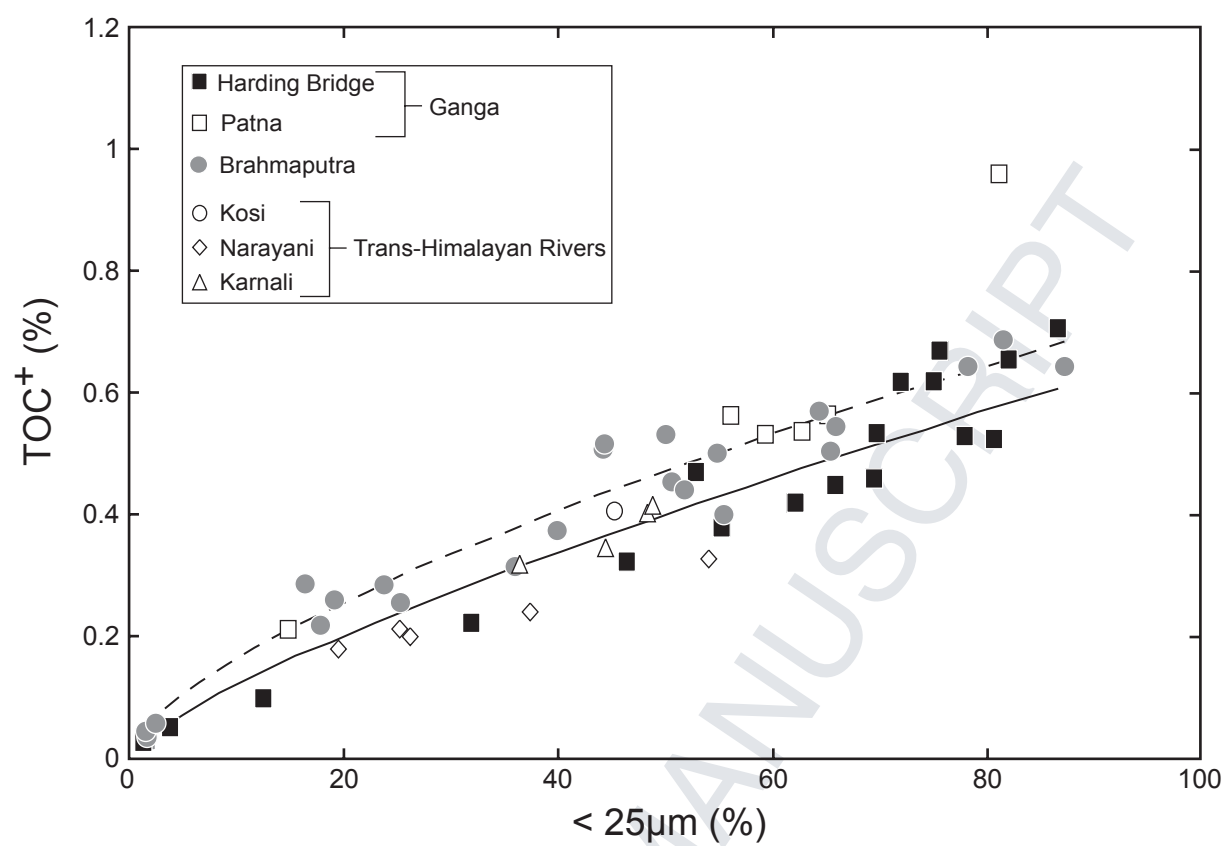


Figure 7

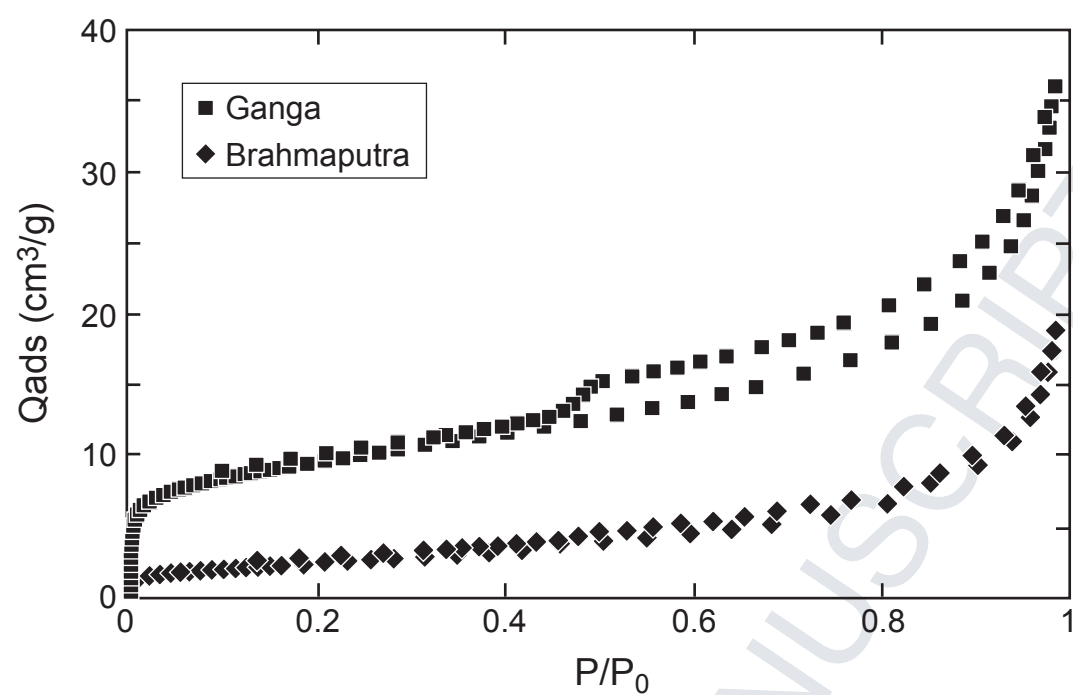


Figure 8

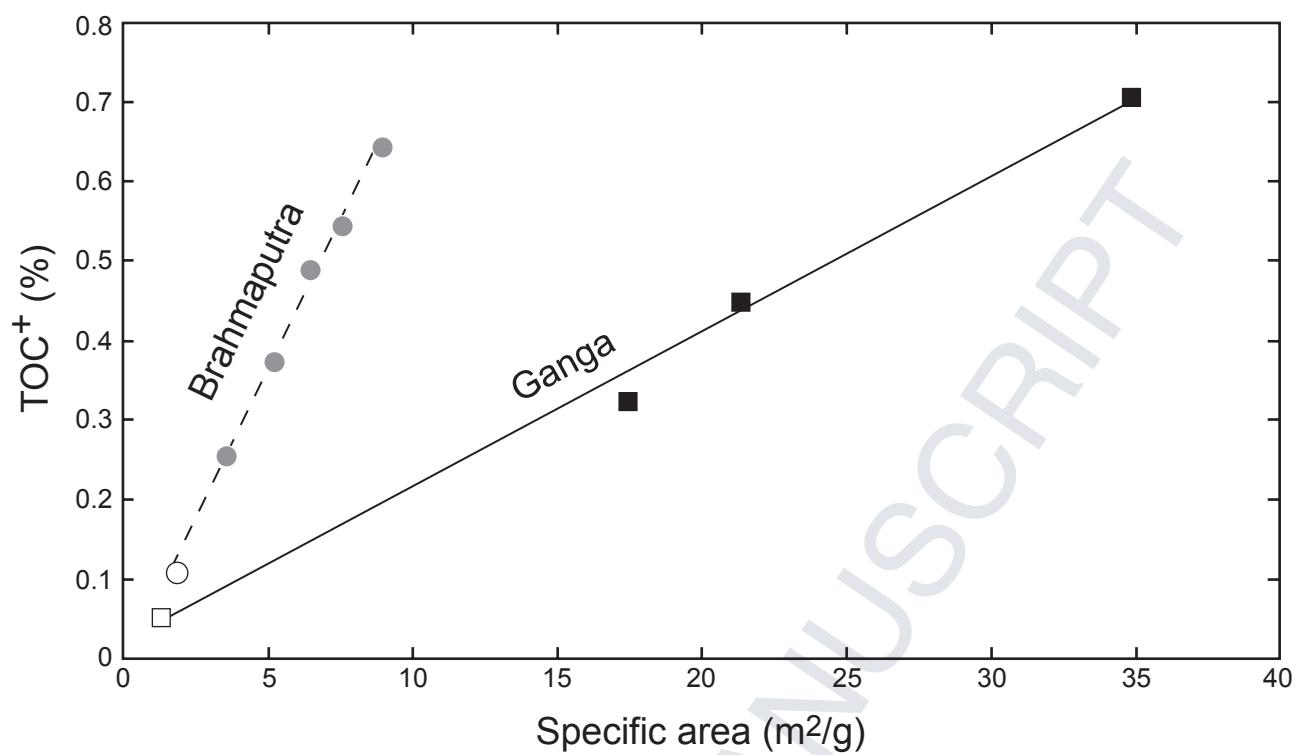


Figure 9

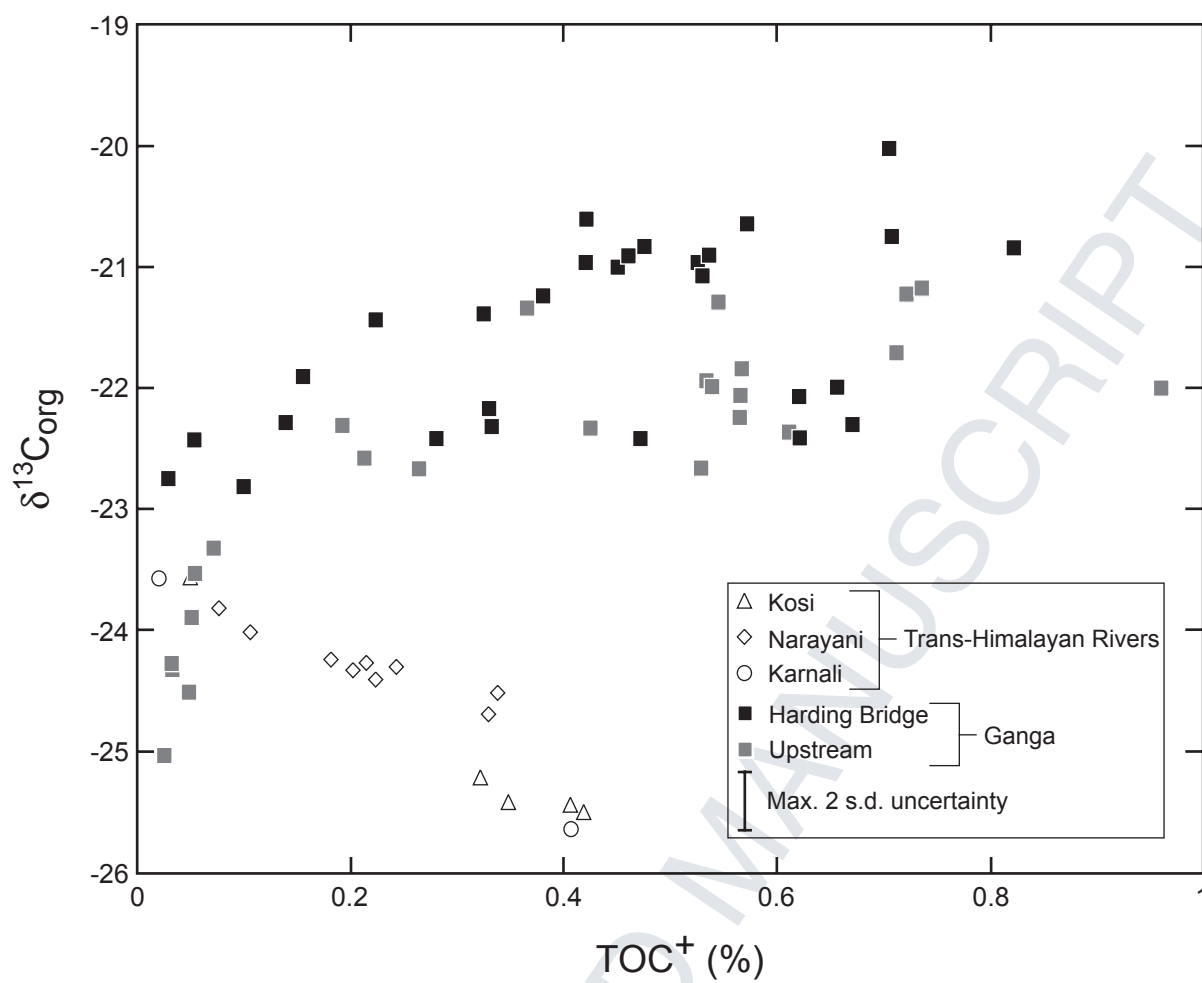


Figure 10

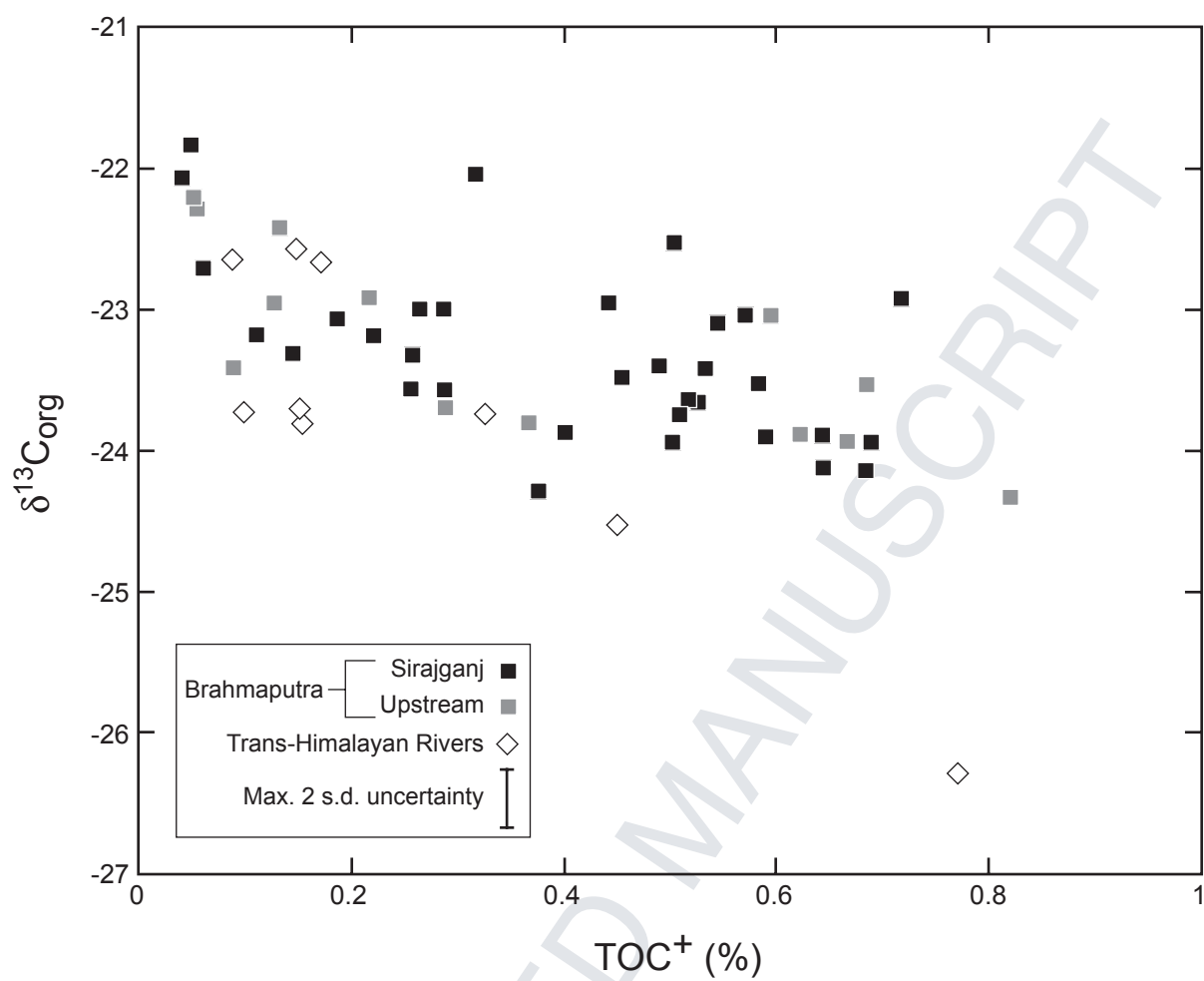


Figure 11

